UNIVERSIDAD DE INGENIERÍA Y TECNOLOGÍA UTEC

Carrera de Ingeniería de la Energía

EFFECTS OF SIGRACET® GAS DIFFUSION LAYERS, WITH DIFFERENT POROSITY AND HYDROPHOBIC AGENT, ON THE PERFORMANCE OF LOW PLATINUM LOADING PEM FUEL CELLS

Tesis para optar el título profesional de Ingeniera de la Energía

Elena Ezquerra Silva

Código 201620041

Asesor

Julien Noel

Lima – Perú

Diciembre 2019

La tesis

EFFECTS OF SIGRACET® GAS DIFFUSION LAYERS, WITH DIFFERENT POROSITY AND HYDROPHOBIC AGENT, ON THE PERFORMANCE OF LOW PLATINUM LOADING PEM FUEL CELLS

Ha sido aprobada

[Nombres y apellidos del Presidente de Jurado]

Julien Noel

[Nombres y apellidos del Tercer jurado]

Dedication:

To my family and my professors.

Acknowledgments:

I would like to thank to all my professors for guiding me through the learning process and for giving me the necessary tools for being an engineer that will contribute to the construction of a more sustainable future. To my supervisor Julien Noel for his support during these years and UTEC, which has been my academic home. To Dr. Marc Secanell, and University of Alberta for awarding me the opportunity of conducting a research internship at the ESDLab, where I was able to learn about fuel cells and conduct the experiments for this thesis. Finally to my family for their unconditional support and for being my daily motivation. None of this would be possible without them.

CONTENT TABLE

Page

CHAPTER I: THEORETICAL FRAMEWORK

CHAPTER II: METHODOLOGY

CHAPTER III: RESULTS

CONCLUSIONS

REFERENCES

ANNEXES

INDEX OF TABLES

Page

INDEX OF FIGURES

INDEX OF ANNEXES

ABSTRACT

This thesis studied the performance of low platinum loading proton exchange membrane fuel cells that were fabricated using the inkjet printing method and assembled with four different types of SIGRACET® gas diffusion layers (28 BC, 29BC, 28 BA and 29BA). The performance was study based on the results obtained from polarization curves, cyclic voltammetry and limiting current experiments. As the major voltage losses of low Pt-loading proton exchange membrane fuel cells are on the mass transport region because of water management problems, the addition of micro porous layers on the gas diffusion layers can prevent the flooding of the cell because of the presence of a hydrophobic agent on the micro porous layer.

The differences between the gas diffusion layers tested are porosity (28-29) and the presence of a hydrophobic agent (BA-BC). The obtained results suggest that the presence of a micro porous layer on the gas diffusion layer is predominant when comparing the performance of the cells with 28BC and 29BC gas diffusion layers, therefore the porosity in this type of gas diffusion layers does not affect much the performance. On the other hand, the gas diffusion layers without micro porous layer, the BA series, show great difference on the performance, being the cell with the gas diffusion layer 28BA with an excellent performance, even better than the BC series, reaching up to 4 A/cm^2 at wet conditions. However, the 29BA gives the worst performance. Despite the outstanding performance obtained with the 28BA, the lack of a micro porous layer on the gas diffusion layer led to a huge crossover because of the carbon fibers intrusion into the catalyst coated membrane. In addition, an improvement on the fabrication process of the cell was achieve adding a drying time of 90 seconds between each layer during the inkjet printing, which allowed reducing the cracks generated on the catalyst coated membrane.

KEY WORDS:

Hydrogen fuel cells; Inkjet printing; Membrane electrode assembly; Low platinum loading; Polymer electrolyte membrane.

RESUMEN

La tesis estudia el desempeño de celdas de hidrógeno del tipo membrana de intercambio protónico que operan con una baja carga de platino. Las celdas se fabricaron usando el método de impresión por inyección de tinta y se ensamblaron con cuatro tipos diferentes de capas difusoras de gas de la marca SIGRACET® (28BC, 29BC, 28BA y 29BA). El rendimiento fue estudiado en base las curvas de polarización, voltametría cíclica y corriente limitante. Dado que las mayores pérdidas de voltaje en las celdas de este tipo se dan en la región de transporte de masa y son debidas a la falta de un manejo adecuado del agua generada; la adición de capas micro porosas en los capas difusoras de gas puede prevenir que la celda se inunde, ya que en las capas micro porosas se encuentra un agente hidrofóbico.

La diferencia entre las capas difusoras de gas testeadas son la porosidad (28-29) y la presencia de un agente hidrofóbico (BA-BC). Los resultados obtenidos sugieren que la presencia de capas micro porosas en la capa difusora de gas es predominante cuando se compara el rendimiento de las celdas con las capas difusoras de gas 28BC y 29BC; por lo tanto, la porosidad en este tipo de capa difusora de gas no afecta mucho el rendimiento. Por otro lado, las capas difusoras de gas sin capas micro porosas (serie BA), muestran una gran diferencia en el rendimiento, al ser la celda con la capa difusora de gas 28BA la que tiene un rendimiento excelente, incluso mejor que la serie BC, alcanzando hasta 4 A/cm^2 en condiciones húmedas; sin embargo, el 29BA muestra el peor rendimiento. A pesar del rendimiento sobresaliente obtenido con el 28BA, la falta de capas micro porosas en la capa difusora de gas condujo a un cruce de protones y electrones a través de la membrana debido a la intrusión de las fibras de carbono en la membrana y en las capas de catalizador. Adicionalmente se lograron mejoras en el proceso de fabricación agregando un tiempo de secado de 90 segundos entre capa y capa durante la impresión por inyección de tinta, lo cual permitió reducir las fracturas generadas en las capas de catalizador que cubren la membrana.

PALABRAS CLAVE:

Pilas de combustible a hidrógeno; Impresión a través de inyección de tinta; Ensamblaje de membrana y electrodos; Baja carga de platino; Membrana de intercambio protónico.

INTRODUCTION

All over the world, there is a growing awareness about global warming and there is an increasing concern on reducing the emissions of CO_2 and other greenhouse gases. Therefore, the human civilization is facing one of the greatest challenges of the century: Controlling Greenhouse Gas Emissions (GHG) for minimizing the impact on the environment [1]. Based on it, in 1997, the Kyoto Protocol promoted by the United Nations Framework Convention on Climate Change (UNFCCC), established the main goal of stabilizing the greenhouse gas concentrations present on the atmosphere avoiding dangerous anthropogenic interference with the climate system [2]. However in the following years no major actions where done for achieving this goal and the effects of climate change became more noticeable. Therefore in 2015, at the 21st Conference of the Parties (COP 21) of the UNFCCC, 196 state parties negotiated the Paris Agreement, where a long term goal was established for keeping the increase in global average temperature to below 2 °C above pre-industrial levels; and to limit this increase to 1.5 °C [3].

Based on the Paris Agreement, many countries started to implement action plans. For example, France announced a plan to ban all petrol and diesel vehicles by 2040, Norway is going to ban the sale also of those types of vehicles by 2025; the Netherlands will do the same by 2030. Now in Germany electric trains powered by wind energy are running on the national rail network [4]. As shown in **Figure 1¡Error! No se encuentra el origen de la referencia.**, the energy sector, in the whole world, is responsible for more than the 60% of GHG emissions [5].

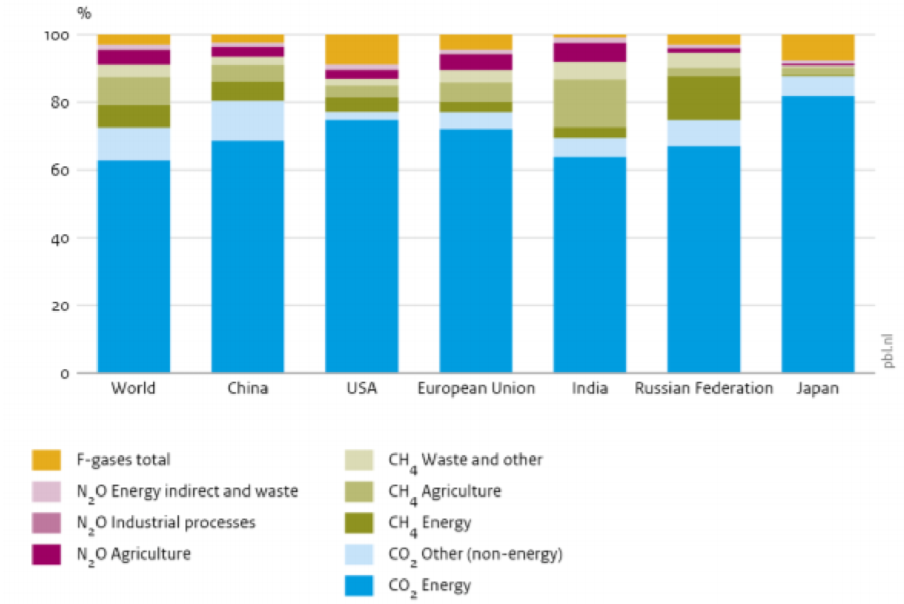

Figure 1 Contribution to 2016 GHG emissions per emission category.
Source: IEA. Trends in global CO_2 and total greenhouse gas emissions [5].

We own alternative technologies that can allow us to replace the current technology used on the energy sector. On one hand, renewable energies avoid CO_2 emissions by replacing fossil fuels in the power generation sector, mainly in conventional thermal power plants. On the other hand, electric vehicles avoid the tailpipe emissions of internal combustion engines of the conventional vehicles [6].

The energy sector is very complex and plays a significant role in our daily life. Worldwide, the CO_2 emissions generated only by the transport sector, as a subsector of the energy sector, represents one of the most significant amounts of emissions. For example, in 2016 the transport sector contributed 24 % of total EU-28 GHG emissions [7]. **Figure 2** shows that fuel combustion used for the transport sector is the second most important source of GHG emissions [7].

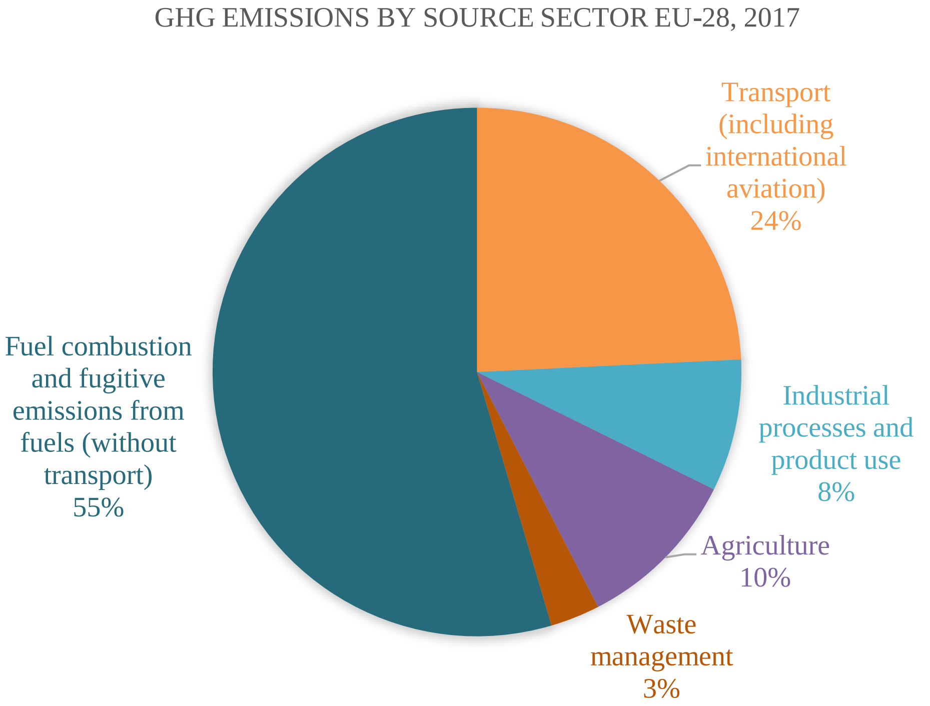

Figure 2 GHG emissions by source sector EU-28, 2017.
Source: Eurostat. Greenhouse gas emission statistics-emission inventories [7].

The same happens in the U.S., transportation accounted for the largest portion (28%) of total U.S. GHG emissions in 2017; according to the Inventory of U.S. Greenhouse Gas Emissions and Sinks 1990-2017 (The national inventory that the U.S. prepares annually under the UNFCCC) [8]. In **Figure 3** it is shown the U.S. GHG Emissions by Sector for 2017. Furthermore, in the same year, for the CO_2 emissions across sectors, transportation accounted for 15% of Asian emissions [9].

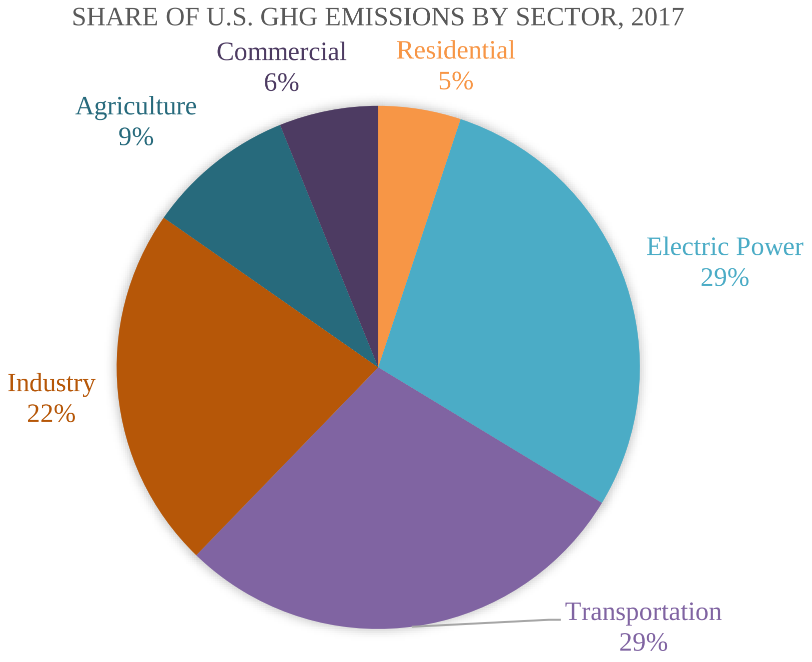

Figure 3 Share of U.S. GHG Emissions by Sector, 2017.
Source: Environmental Protection Agency. U.S. Transportation Sector Greenhouse Gas Emissions [8].

Therefore, the transport sector is one of the greatest responsible of GHG emissions all over the world, and only light-duty vehicles, in the U.S. for example, generate one-third of total CO2 emissions from the country [10]. As it is effectively impossible to capture CO_2 emissions from individual vehicles, the only way of reducing the emissions in the transportation sector is by replacing current fuels with lower carbon fuels or even better, with zero-carbon vehicles [10].

A sustainable alternative to the vehicles with an internal combustion engine, are the battery and fuel cell electric vehicles (Hereafter BEVs/FCEVs), as long as the electricity and hydrogen are generated from renewable energy sources [6]. EVs are already been developed and play an important role in the energy transition. Their massive implementation will allow us to achieve the reduction of global CO2 emissions.

The proton exchange membrane fuel cell (PEMFC) is the type of fuel cell most widely used for transport applications; however, this technology still cannot be massively implemented because of the lack of hydrogen infrastructure (fueling stations), the high production cost of this technology and technical limitations. In order to overcome these problems, the first goal was to reduce the platinum loading in order to reduce the production costs; after achieving it, mass transport losses at high current densities become a performance and durability problem.

In that regard, the current thesis focuses on identifying the type of Gas Diffusion Layer (GDL) that contributes to solve the problem of mass transport losses and gives higher performance to low platinum loading Proton-Exchange membrane fuel cell (PEMFC). In order to achieve it, there will be fabricated low Pt-loading PEMFC using the inkjet printing method and then the cells will be assembled with different GDLs and connected to a fuel cell station where polarization curves, cyclic voltammetry tests and impedance spectroscopy tests will be run in order to study the performance of cells.

Scope

The scope of this thesis is to fabricate, assemble and test single PEM fuel cells with different SIGRACET® gas diffusion layers (28 BC/29 BC/28 BA/29 BA). Then, study the performance of the different cells and determine the effects of the GDL porosity and the presence of a micro porous layer (MPL) on the fuel cell performance.

The fabrication and testing of the fuel cells will take place at the Energy Systems Design Laboratory, University of Alberta, Canada. The method that will be used for the fabrication of the catalyst-coated membrane is the inkjet printing method and the ink will be prepared with platinum powder supported by carbon, Nafion®, and a solvent mixture. The printer used for printing the catalyst layers over the membrane is the FUJIFILM Dimatix printer. Then the cells will be assembled and tested on the 850e Multi-Range Fuel Cell Test System, in order to obtain polarization curves, cyclic voltammograms, and resistance values with the FuelCell® software.

Background

Nowadays, a potential EV driver can choose between a battery-powered electric vehicle and a hydrogen powered fuel cell electric vehicle. Each of these technologies has its own advantages and disadvantages regarding cost, range, performance, and infrastructure, as shown in **Table *1***, those are some of the differences between BEVs and FCEVs.

Characteristic	BEV	FCEV
Recharging/Refueling infrastructure	80% charging could be at home, chargers are easier to install	Too complex the implementation of a hydrogen recharging network
Recharging/Refueling speed	Low	Fast as ICV
Range	Limited by power density of batteries	As good as ICVs
Energy demand	18-25 kWh of electricity per 100 km	60 kWh Electricity-H_2-electricity
Flexibility to follow intermittent Renewable Energy Systems (RES)	Has to be connected to the power grid in times of high RES generation	H_2 can be generated any time and be easily storage
Round-trip efficiency	>70%	40-60%

Table 1 Differences between BEV and FCEV.
Source: Own elaboration based on [6][11][12].

Currently there is no clear answer as to which one could dominate the future low carbon vehicle market. However, there are various technical, economic and infrastructural barriers that limit the large scale adoption of both the FCEVs and BEVs [13]. Both types of vehicles share many of the same components because they operate with the same electric system inside the EV; they both have an electric motor and power controller or inverters; however, their main energy source, their input, is very different. Hydrogen Fuel Cell Vehicles (HFCVs) use a fuel cell to convert the hydrogen energy into electricity and BEVs use batteries to storage the energy [14].

In the future, both of these technologies will probably coexist, while the BEVs are more suitable for short range and small vehicles, the HFCEVs are mostly to be applied in medium and long range vehicles [15]. By 2050, BEVs and FCEVs could become less expensive than the advanced Internal Combustion Engine Vehicles (ICEVs). Putting aside the complexity of developing a hydrogen infrastructure, fuel cell vehicles are the most promising alternative to ICEVs mainly because they are not subject to the limitations of battery vehicles [10]. Nevertheless, why are there less than 10 thousand of hydrogen vehicles running all over the world?

First, the production cost a hydrogen fuel cell vehicle is still too high for being a competitive technology as internal combustion engines vehicles. On 2017, a team from the Department of Energy, Argonne National Laboratory, made an analysis on the cost of direct hydrogen fuel cell vehicles. They found that the estimated system cost to date for 100,000 and 500,000 units per year, result in a total system cost of 50$/kWnet and 45$/kWnet, respectively. For 2025, there is a target of a total system cost of 40$/kWnet and the ultimate goal is to reduce the overall HFCEVs system to 30$/kWnet in order to be on a essentially cost parity with ICEVs [16].

Second, there has been less research and technology improvements for FCEVs than for BEVS. Over the past decade, there had been very significant cost reductions and performance improvements of Li-ion battery packs for EVs, making the BEVs a more competitive technology available in the market [17]. As shown in **Figure *4***, between 2010 and 2016 the battery costs had been reduced on 77%, being now near to reach the $125–$150 target that makes EVs competitive with conventional gasoline vehicles [18]. On the other hand, as shown in **Figure *5***. between the same period of time (2010-2016), the costs of fuel cell systems had been reduced only on a 17%, being now still far from the target of 30$/kW for being as competitive as ICEVs.

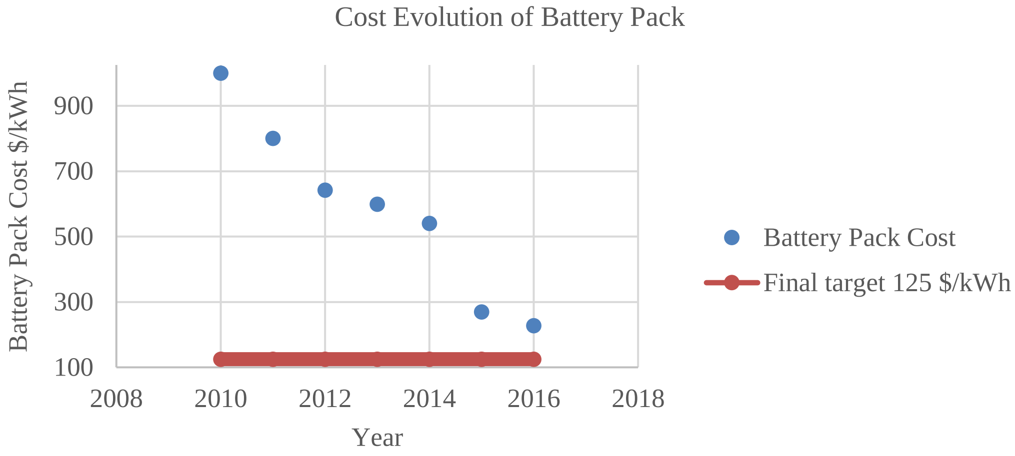

Figure 4 Cost Evolution of Battery Pack for EVs (2010-2016).
Source: Own elaboration based on [18][19].

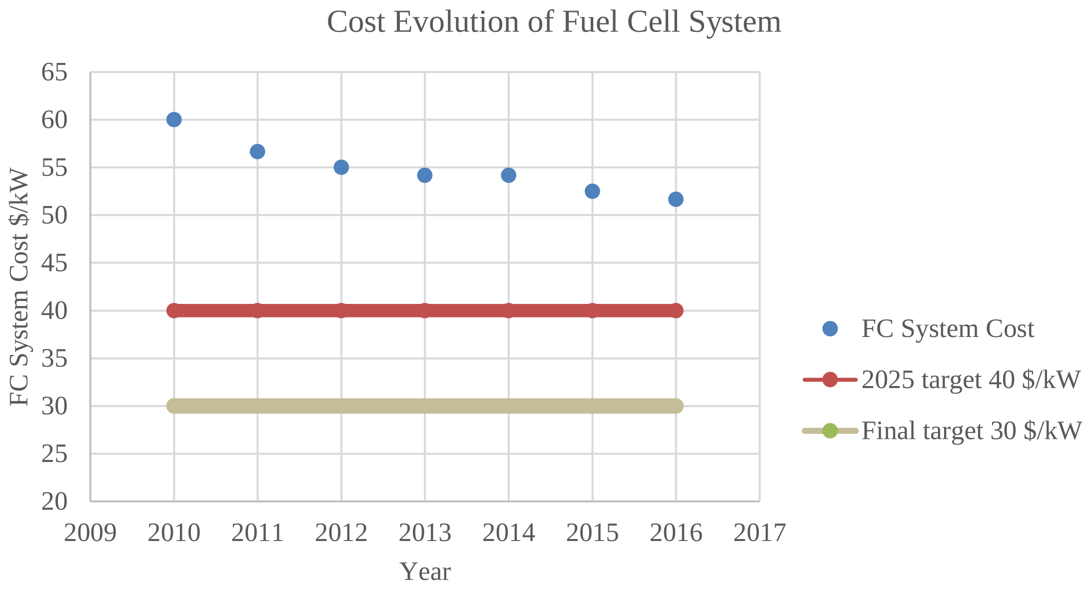

Figure 5 Cost Evolution of Fuel Cell System for EVs (2010-2016).
Source: Own elaboration based on [16] [20].

Third, as shown in ***Figure 6***, the greatest cost of the Fuel Cell Stack is represented by the membrane electrode assembly (MEA), and inside of it is the catalyst component that represents 41% of the overall cost. The catalyst used on PEMFC is platinum, a precious metal that is rare and expensive [21].

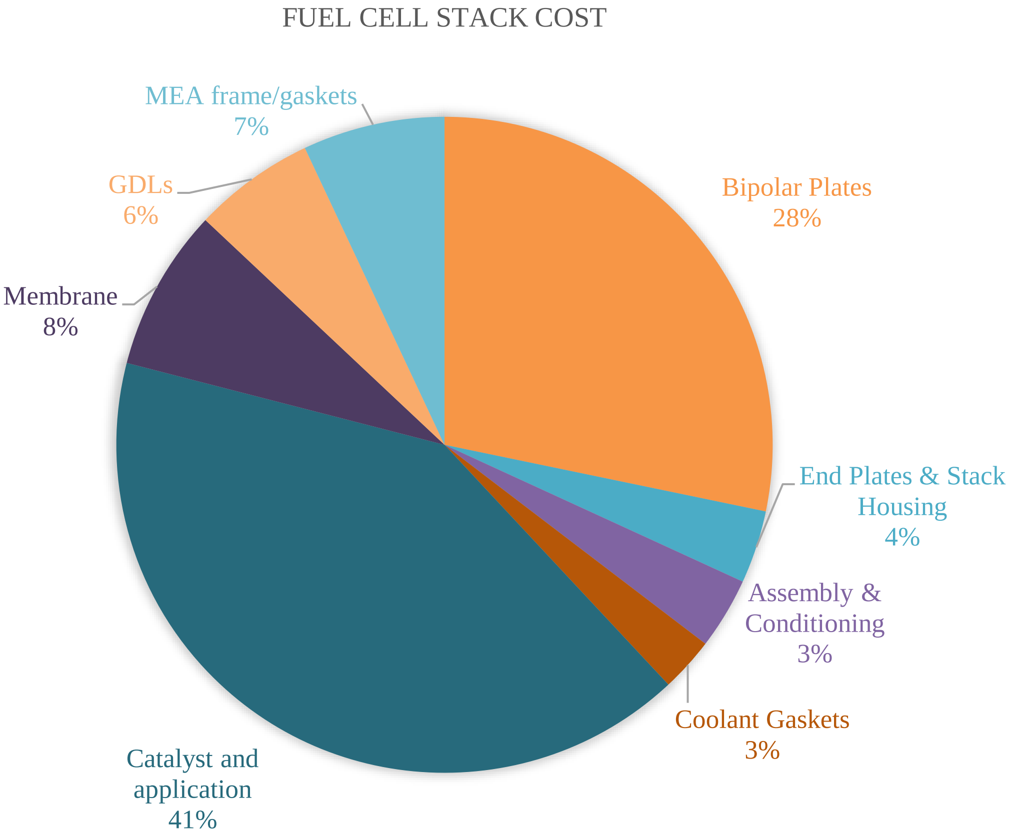

Figure 6 Component cost breakdown at production volume of 5M units/yr for the FC stack Source: Thompson et al. Direct hydrogen fuel cell electric vehicle cost analysis: System and high-volume manufacturing description, validation, and outlook [16].

In order to achieve a massive penetration of these type of vehicles into the market, they need to be as cost effective as today's ICEVs so that they can be more competitive and widely commercialized. Based on the research that has been done so far, still more research has to be done in order to achieve a cost reduction in materials, especially in the catalyst area. The last years, the researchers have been focused on reduction of platinum group metal (PGM) content, platinum alloys, novel support structures, and non-PGM catalysts. Given that the catalyst cost is projected to be the largest contributor to overall system level costs at high volume production, if we achieve substituting the platinum with an alternative material that still works as a catalyst, then the overall cost of the system could be reduced [22].

Justification and Motivation

In the past few years there have been significant improvements in the development of FCEVs, however further development of this technology has to be done because they are still not as efficient and cost effective as ICEVs are. According to The National Research Council, one of the main technology challenges for the HFCV is making the fuel cell system as durable and cost effective as today's conventional engines for vehicles [10]. In addition, the Committee on Transitions to Alternative Vehicles and Fuels states that the research done on advanced materials and battery concepts will be critical for the success of electric drive vehicles. It also recommends that the following research areas will have the greatest impact [23]: New catalyst structures that increase and maintain the effective surface area of chemically active materials and reduce the use of precious metals. And the development of novel structures of gas diffusion layers that maintain an effective amount of water and increase the performance and durability of fuel cell stacks.

One of the laboratories that is working on the development of fuel cells and sustainable electrochemical systems is the Energy Systems Design Laboratory at University of Alberta, Canada. In the past years, this research team has achieved to reduce the platinum loading using in-house inks based on platinum supported by carbon and coating the catalyst over the membrane with the inkjet printing method [24]. Nowadays, they are working with low-Pt loading PEM fuel cells, however after achieving high current densities with less platinum loading; the water management has become a major problem.

There has been identified mass transport loses that affected the performance of the cells because of the water accumulation on the cathode side at high current densities. The proton conductivity is directly proportional to the amount of water generated, and a higher proton conductivity gives a better performance however, high levels of water is not desired. There should not be so much water because if the electrodes that are bonded to the electrolyte flood, the pores in the electrodes or the GDL will be blocked, disabling the proton exchange. A balance is therefore needed, which takes a lot of effort to achieve [25].

One of the components of the fuel cells is the gas diffusion layer which serves as structural support and electrical conductor, and this component with an appropriate porosity and with a hydrophobic agent, may help to solve the mass transport problem [26].

Therefore, this thesis will study the effects of SIGRACET® GDLs on the performance of the PEM fuel cells. The aim of this research project is to contribute to the elaboration of more scientific knowledge on low Pt-loading PEMFC because the achievement of improvements on the performance of this technology will allow us to turn it into a more competitive technology and replace internal combustion engines. Moreover, achieve to scale-up the use of FCEVs in the market would subsequently accomplish the overall objective of reducing CO_2 emissions worldwide, contributing to the construction of a more sustainable transport sector.

General Objective

Study the effects of SIGRACET® gas diffusion layers with different porosity and hydrophobic agent on the performance of low Pt-loading PEMFC.

Specific Objectives

- Study the performance of low Pt-loading PEMFC and identify major losses.
- Perform a literature review and identify a solution to the problem previously identified.
- Investigate and identify the properties of SIGRACET® gas diffusion layers (28 BC/29 BC/28 BA/29 BA).
- Fabricate PEM fuel cells using the inkjet printing method.
- Assemble and test single PEMFC with different SIGRACET® GDLs.
- Study the effects of different SIGRACET® GDLs on the performance of PEMFC.

CHAPTER I

THEORETICAL FRAMEWORK

In the late 1900s, the concept of the fuel cell emerged as a new electrochemical power device. Since then, many scientists and engineers believe that fuel cells hold promise as an alternative energy source to help offset our traditional reliance on coal, oil, and natural gas [27]. However, it was in 1839, the first discovery of the fuel cell principle by William Grove, a lawyer and physicist from Great Britain [28]. Nevertheless, it was until 1960s, in the Apollo space program, that the fuel cells where used to power the onboard electrical systems of the Apollo spacecraft. They were use because no batteries could last long enough for a flight to the moon; the system provided both, electricity and drinking water for the astronauts. This energy device supplied 1.5 kW of continuous electrical power over ten thousand hours of operation, without a single in-flight incident [29].

Besides that, the performance of fuel cells that NASA deployed was exemplary, the cost per kilowatt was astronomical because the FC were hand-built and used exotic materials. Therefore, other types of technologies emerged with a higher commercial potential, and research of FC continued at a low funding level [28]. It was recently at the beginning of 1980s, when governments agencies in the US, Canada and Japan, significantly increased their efforts on the development of fuel cell technology [30].

1.1 Fuel Cell Technology

According to the U.S. Department of Energy, a fuel cell is an electrochemical device that converts the chemical energy of hydrogen or another fuel to electrical energy in a cleanly and efficiently way [16]. Unlike batteries, the energy supply in a fuel cell is external and can be supply essentially indefinitely by refueling the external tank, the same as in an internal combustion engine.

Generally, fuel cells use gaseous or liquid fuels, such us natural gas, methanol, etc., but hydrogen fuel cells uses hydrogen as fuel and the oxidant for a fuel cell is usually oxygen in air [31]. In comparison to heat engines, the energy conversion in fuel cells is direct and simple and it is not limited by thermodynamic limitations like Carnot efficiency [32].

Fuel cells are a promising technology for the transportation, power generation and even as an energy storage device because of their high energy density and efficiency and low environmental impact [33]. They are very versatile because can be used as very small devices producing only a few watts of electricity, or as large power plants producing megawatts. Fuel cells are suitable for different applications because there are different types. These are classified according to the nature of the electrolyte they use, each type require particular materials and uses different fuels and reactants [34]. As shown in **Table 2** fuel cells have advantages and disadvantages when compared to internal combustion engines and batteries. Those disadvantages are the reason why still this technology cannot massively replace other technologies with lower efficiency and higher impact on the environment, however these limitations eventually will be solved by the development of research and engineering solutions [35].

Advantages	Disadvantages
Higher efficiency: direct production of electric energy (40-50%)	Lack of hydrogen infrastructure, is difficult to produce and store hydrogen
Low chemical, acoustic and thermal emissions (have no big moving parts and GHG emissions are low if hydrogen is used as fuel)	Emerging technology that still needs to accomplish reductions in cost, weigh, size, and increase in reliability and durability.
Fuel flexibility: it can be used hydrogen, natural gas, propane, and even anaerobic digester gas	Require relatively a pure fuel, without contaminants that can deactivate the fuel cell catalysts. Therefore, in some cases is needed a reformer on the fuel cell system.
Compactness: higher energy density and energy storage capacity. Fuel cell system is lighter than batteries.	Fuel cell system is still a little heavier than internal combustion engine systems
Exhibit good load-following characteristics because are solid-state devices that react chemically and instantly to changes into load.	
Don’t need recharging, they must be refueled, which is faster	
Modularity: allow independent scaling between power and capacity. The fuel cell size can be adapted by simply changing the number of fuel cells stacks.	

Table 2 Advantages and disadvantages of fuel cell technology
Source: Own elaboration based on [30][36][35].

1.1.1 Basic operation principles

A fuel cell consists mainly of an anode, an electrolyte, and a cathode. As shown in Figure 7**¡Error! No se encuentra el origen de la referencia.**, on the anode side, the fuel is oxidized electrochemically and releases positively charged ions; on the cathode side, oxygen molecules are reduced to oxide or hydroxide ions [37]. The electrolyte is the medium through which either the positively charged ions travel from anode to cathode or the negatively charged ions travel from cathode to anode. The only byproduct that goes out of the system is water vapor. A catalyst is often used to speed up the electrochemical reactions at occur on the electrodes [34].

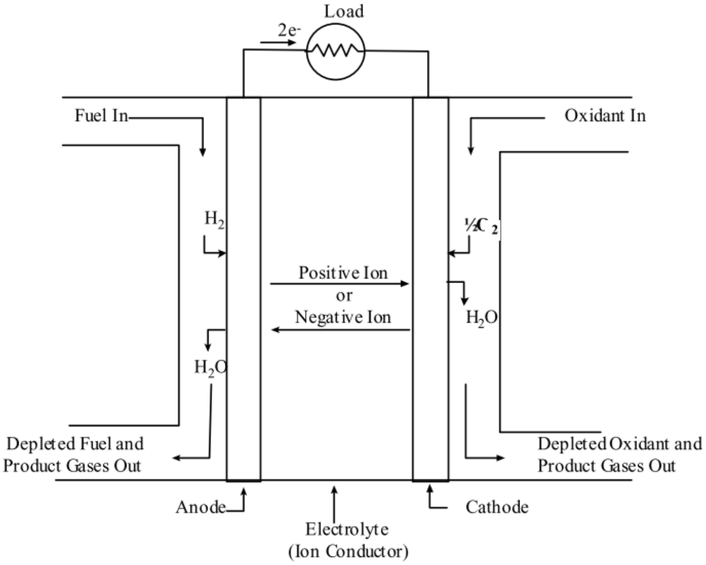

Figure 7 Basic schematic fuel cell operation
Source: Nail et al, The Evolution of the PEM Stationary Fuel Cell in the U.S. Innovation System [38].

The reactants of fuel cells can be classified based on the properties of the components that donate the electron (oxidant) or accept the electron (reductant). Oxidants mainly include pure oxygen and the reductants, which are also known as the fuels, include pure hydrogen or gases that contain hydrogen like ethanol, methanol, natural gas, etc. [39]. The most basic reaction that occur inside the fuel cell consists of the combustion of hydrogen fuel into water, and this process is split into two electrochemical reactions: the oxidation reaction (1) that occurs on the anode and the reduction reaction (2) that occurs on the cathode. These are the two half reactions and the overall combustion reaction is given by the combination of the two half reactions (3) [40].

$$H_2 \rightarrow 2H^+ + 2e^- \quad (1)$$

$$\tfrac{1}{2}O_2 + 2H^+ + 2e^- \rightarrow H_2O \quad (2)$$

$$\tfrac{1}{2}O_2 + H_2 \rightarrow H_2O \quad (3)$$

The role of the electrolyte is to contain the two half reactions electrically while allowing the movement of ions: the protons produced at the anode are moved to the cathode side where they will combine with the oxygen and form a molecule of water [32]. Therefore, electrolytes should be both good proton conductors and excellent electric insulators. There is a third requirement for electrolytes, they need to be impermeable to gases so that the anodic and the cathodic compartments remain separated, in order to prevent gas crossover [34]. Through the electrolyte, the flow of electrons is hindered; therefore, it is forced to go through another way. There should be an external electrical circuit through which the electrodes flow and that allows fuel cells to provide DC power by the direct collection of electricity [41].

In the case of the electrodes, a high surface area is an important feature in order to maximize each half reaction zone, for this reason they are relatively porous compounds [42]. According to the application of fuel cell technologies, the materials of the whole systems depends on each type of fuel cell and they are describe on the section below. Every type of fuel cell is characterized by its own particular dimensions, reactants and materials; however the basic structure of fuel cells consists of an electrolyte, two electrodes, and requires a fuel and a oxidant for producing electricity [43].

1.1.2 Types of Fuel Cells

Nowadays, there are different types of fuel cells that are currently under development and are classified primarily based on the electrolyte they use. The electrolyte is an essential part of the fuel cells, and it determines the operating parameters, such as the type of catalysts, the electrochemical reactions, the operating temperature, the reactants that can be used and therefore the applications for which these cells are most suitable [44]. The most promising types of fuel cells, with their characteristics, are show in **Table 3**. The schematic fuel cell operation of each type can be find on **Annex *1***, **Annex *2***, **Annex *3***, **Annex *4***, **Annex *5***, and **Annex *6***.

Fuel cell type **Operation temperature** **Efficiency**	**Common Electrolyte** **Charge carrier** **Fuel** **Electrode catalyst**	**Applications**
Polymer electrolyte membrane (PEMFCs) 50-100 °C 60%	Perfluorosulfonic acid H+ Hydrogen Platinum based	Distributed generation Portable power Transportation Ideal for vehicles
Direct methanol (DMFCs) 60-130 °C 60%	Perfluorosulfonic acid H+ Methanol Pt-ruthenium	Portable power Early market applications
Alkaline electrolyte (AFCs) 50-100°C 60%	Alkaline polymer, aqueous KOH OH^- Pure hydrogen Nickel	Portable power Backup power Space shuttles
Phosphoric acid (PAFCs) 150-250 °C 40%	H_3PO_4 H^+ Hydrogen Pt catalyst dispersed on carbon	Distributed power
Molten carbonate (MCFCs) 500-700 °C 45-50%	$(Li, K, Na)_2CO_3$ CO_3^{2-} Hydrocarbon fuels (methane) Non-precious metal	Distributed power Electric utility
Solid oxide (SOFCs) 600-1000 °C 60%	Stabilized Zirconia Oxides O^{2-} Hydrocarbon fuels (methane) Non-precious metal	Distributed power Electric utility APUs

Table 3 Types and characteristics of fuel cells
Source: Own elaboration based on [31][32][33][34][35][45][46].

1.1.3 Application of fuel cells on transportation

One of the most common application of fuel cell technology is on the transport sector. In addition to the environmental advantages offered by fuel cells, they have several properties that make their use suitable for many transport applications, including scooters, passenger cars, busses, and even space shuttles [43].

FCEVs are considered low emission vehicles and the HFCEVs zero emission, these vehicles have greater efficiency than ICEVs and BEVs [47]. This type of vehicle propulsion system has short startup times, high dynamic load demand and requires to operate at low temperatures, therefore, PEMFCs are the technology most widely used for this application [36].

The transportation application of FCs is mainly concentrated on automobiles, buses and niche transport applications [48]. The development and application of PEMFC in the transport sector is competitive and promising due to the desire of depleting fossil fuels and the need of zero emission vehicles. Currently most of the governments (like USA and Japan) and the companies car makers are actively engaged on the development of this technology and are working on the onboard integration of fuel cell systems and electric energy storage devices with an energy management system [35].

The main components and the basic operation of a hydrogen fuel cell vehicle are show on **Figure 8** where the letter A represents the electric motor, the letter B the fuel cell stack, C is the battery and D is the high-pressure hydrogen tank. On the first step, the oxygen present in the air gets into the system. Then on step 2, the oxygen and hydrogen supplied to fuel cell stack. The third step is the generation of electricity and water, through the electrochemical reaction produce inside the fuel cell stack. On step 4, the electricity generated feed the electric motor and then, step 5, the motor is activate and powers the vehicle system, enabling it to move. The last step, step 6, is the water expulsion of the outside the vehicle as tailpipe emission [49].

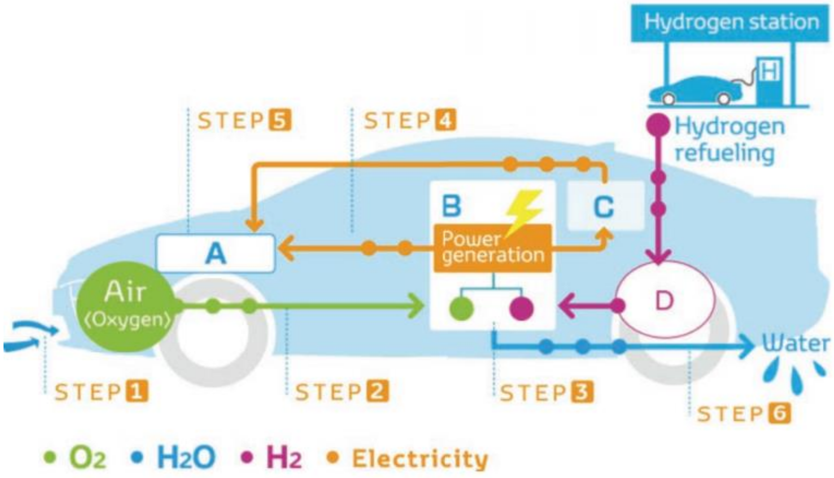

Figure 8 HFCEV operation diagram
Source: N. Barilo and S. Loosen, Hydrogen Fuel Cells and Fuel Cell Electric Vehicles [49].

1.1.4 Evolution of hydrogen fuel cell electric vehicles technology

Today, passenger cars powered by fuel cells have demonstrated about 3000 hours of operations (depending on speed: 150-300 thousands kms), but still durability issues like start-stop operation and steep transient load cycling, have to be solved. However, the major problem are the high costs despite the significant cost reduction achieved over the last years [50].

The automobile manufacturers that are currently leading the development of HFCEVs in the United States, are Daimler and Ford; there is also the Automotive Fuel Cell Cooperation (AFCC) with Ballard [51]. On 2013, the companies Daimler AG, Ford Motor Company and Nissan Motor Co. signed an agreement where the three parties agreed for a joint development of common fuel cell system to speed up the development of the technology, furthermore increase the availability of zero-emission technology and significantly reduce costs [52]. In Japan, the largest auto manufacturers are Toyota, Honda and Hyundai [40].

Despite all the efforts of the governments and companies put on the development of FCEVs, today still these type of vehicles are not massively available on the market, many of them are still prototypes units [36]. Nevertheless, in the last 5 years, fuel cell cars started to come out of demonstration stage and are becoming commercials, by today, companies like Toyota, Hyundai and Honda have started initial commercial sales of their fuel cell cars. In

2013 the first fuel cell vehicle became commercially available and since then until 2017, 6,364 hydrogen fuel cell vehicles were sold globally [53].

The most advance fuel cell vehicle with the world's best fuel cell efficiency and with a driving range of 666 km is the NEXO Fuel Cell SUV. This vehicle can reach a maximum speed of 179 km/h, a maximum output motor of 120 kW, the total output of the fuel cell systems is 135 kW, the stack is conformed of 440 cells (250-450V) [54]. The evolution of the FCEVs of Hyundai is show on **Figure 9**.

1st Generation 2000 - 2004	2nd Generation 2005 - 2008	3rd Generation 2009 - 2011	4th Generation 2012 - 2016	5th Generation 2017
Core Technology Development	System Technology Development & Fleet Operation	Semi-Automatic Production	Pre-Commercial Production (pilot-scale)	Commercial Production
Several FCEVs	Stack Bipolar Plate – Graphite	Stack Bipolar Plate – Metal	1000 FCEVs	Full Automated Production line
	Tens of FCEVs/year	> 100 FCEVs		Several thousand FCEVs

Figure 9 Evolution of FCEVs manufactured by Hyundai
Source: INSIDEEVs, Hyundai Announces Partnership With Audi On Fuel Cell Technology [55].

Because of the high costs and extensive knowledge required for the development of this technology, many companies are joining their forces in order to achieve the massive commercialization of cost-efficient HFCVs [54]. As stated by Mark Kane, a European editor, *"The partnership between Hyundai Motor Group and Audi will leverage collective R&D capabilities in fuel cell technology to elevate their presence in the FCEV market. Therefore, the agreement also includes mutual access to fuel cell components. As a first step, Hyundai Motor Group will grant its counterpart the access to parts that are based on Hyundai's know-how accumulated from the development of ix35 Fuel Cell as well as NEXO. Audi – responsible for the development of fuel cell technology within the Volkswagen Group – will also be able to take full advantage of Hyundai's FCEV parts supply chain. Hyundai Motor Company, the world's first mass*-producer of fuel cell vehicles, has been offering SUV-Class *FCEVs since 2013, and currently sells them in 18 countries around the world"* [56].

Despite the achievements that have been accomplished so far, there are still two major challenges to HFCEVs commercialization, reducing cost and improving durability [57]. Ongoing research is mainly focused on the development of new materials for the membranes, catalysts, bipolar plates and membrane electrode assemblies in order to reduce the cost and extend the life of fuel cell stack components [46].

1.2 Proton Exchange Membrane Fuel Cells

The proton exchange membrane (PEM) fuel cell use an electrolyte that conducts the protons from the anode to the cathode, these electrolyte is composed of a solid polymer film of acidified Teflon [36]. This is the most suitable type of fuel cell for transportation applications. The characteristics that make this type of fuel cell the most widely used on vehicles are the low operating pressures (15-30 psig), which increases the safety of the system and low temperatures (<100°C) that allows relatively short start-up times, and the "load following" that means that it responds almost instantaneously to changing power demands [28].

A PEM hydrogen fuel cell generates approximately 0.7 V DC under no-load conditions. In order to obtain higher voltages, multiple PEM fuel cells can be connect in series. A series-connected set of fuel cells technically forms a battery, but engineers call it a stack [58]. The PEM cell stacks have already been made compact and powerful enough, and they provide power and acceleration equal to, or even better than, internal combustion engines; for this reason, since 1994 FCEV are available in the market being offered by companies like Daimler, Toyota, Nissan, Honda, Hyundai, General Motors, Ford, etc. [59].

This technology has drawn the attention because of its simplicity, viability, suitability, and quick start-up and because it has been even proposed as a promising power source for zero emission vehicles [42]. PEMFC systems are suitable for different vehicle applications since they do not require the use of hazardous fluids, and they enjoy high power densities while maintaining low operating temperatures [35]. It is shown in **Table 4** the advantages and disadvantages of this specific type of fuel cell.

Advantages	Disadvantages
• Tolerant to carbon dioxide • Operate at low temperatures and pressures • Use solid, dry and non-corrosive electrolyte • High voltage, current and power density • Use stable materials • Relatively simple mechanical design • Compact and rugged	• Only tolerate 50 ppm CO • Tolerate few ppm of total sulfur • Use an expensive platinum catalyst • Is difficult to work with the membrane, water management problems

Table 4 Advantages and disadvantages of PEMFCs
Source: Own elaboration based on [36][35][32].

1.2.1 Working principles

Inside a PEM fuel cell, two electrochemical reactions take place and make up the total redox reaction, at the anode an oxidation reaction, loss of electrons, (1) and at the cathode a reduction reaction, gain of electrons (2) [29]. On the reduction reaction the H^+ is drawn through the electrolyte from the anode to the cathode the reactive attraction of hydrogen to oxygen, while electrons are conducted through an external DC circuit [34]. The overall cell electrochemical reaction (3) is obtain combining anode and cathode reactions. The product of the whole reaction is water; this must be continually remove of the system to facilitate the continuity of further reactions. All of this process is better show on **Figure 10**. A Schematic operation of PEMFCs [46].

$$H_2 \rightarrow 2H^+ + 2e^- \quad (1)$$

$$\frac{1}{2}O_2 + 2H^+ + 2e^- \rightarrow H_2O \quad (2)$$

$$\frac{1}{2}O_2 + H_2 \rightarrow H_2O \quad (3)$$

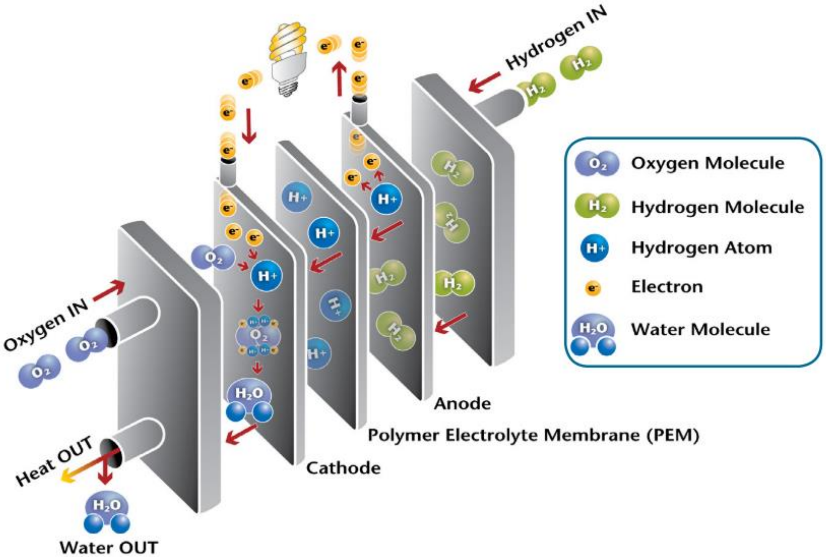

Figure 10 Schematic of a Polymer Electrolyte Membrane fuel cell
Source: U.S. Department of Energy, FUEL CELL TECHNOLOGIES, Energy Efficiency & Renewable Energy [46].

1.2.2 Structure and Components

The main component of a PEM fuel cell is the membrane electrode assembly (Hereafter MEA), which is composed by the membrane, the catalyst layers, and gas diffusion layers (Hereafter GDLs). As shown in **Figure 11**, MEA components are the GDLs, the catalyst layers (Hereafter CLs), and the proton exchange membrane. On one side is an electron-conducting anode consisting of porous GDLs as an electrode and an anodic catalyst layer; on the other side is an electron-conducting cathode consisting of a cathodic catalyst layer and again, a porous GDL as an electrode and in the middle there is a proton-conducting electrolyte, a hydrated solid membrane [44].

Besides the MEA, there are hardware components that incorporate the MEA into a fuel cell and enable an effective operation. These includes gaskets that provide a seal, preventing leakage of gases, they are usually made of rubbery polymer like Teflon (PTFE) [30]. There are also bipolar plates that assemble individual PEMFCs into a whole fuel cell stack and incorporate channels for the fluids, they are usually made of metal, carbon or composite and provide electrical conduction and physical strength to the stack. Finally, outside the cell there are current collectors with the reactant gas flow fields and take the electrons to an external circuit, providing a DC current [60].

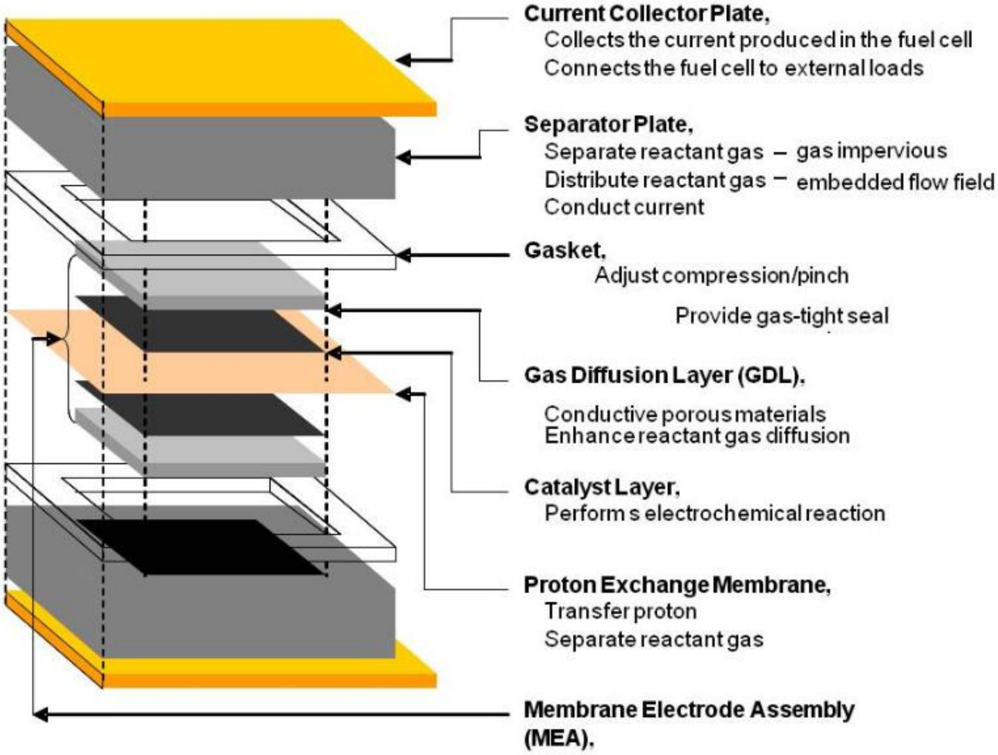

Figure 11 Basic structure and components of the PEMFC
Source: NPTEL, Fuel Cell Technology [61].

The most common membrane used at PEMFC is Nafion (DuPont), a sulphonated polymer, its layer has a thickness between 35 and 170 μm, while thinner is the membrane the cell will have a higher conductivity because there will be less resistance, nonetheless this implies water management problems [35]. The main function of the GDLs is to act as a gas diffuser, which means to provide mechanical support as an electrical pathway for electrons and as a channel for the evacuation of the byproduct, water. Typically are constructed from carbon paper with thickness between 100 and 300 μm [26].

1.2.3 Catalyst Layers

The catalyst layers are where the electrochemical reactions take place; they transport the electrons from the GDLs to reaction site, as well as the protons from the membrane to the reaction site. Usually these layers are made of platinum and the typical thickness of the CLs is between 1 to 20 μm [62].

The nanoparticles of platinum are dispersed on a high surface area supported by carbon for later being mixed with an ion-conducting polymer, usually Nafion [60].

1.2.3.1 Materials

The catalyst layer, is a porous electrode containing carbon-supported platinum mixed with a polymer electrolyte, given that he electrochemical reaction occurs here, the material and structure of the CLs have a major influence on the overall performance of the fuel cell [63]. In order to facilitate the electrochemical reactions, the CLs should meet the following three properties: electronic conductivity, protonic conductivity and gas diffusivity as shown on **Figure 12**.

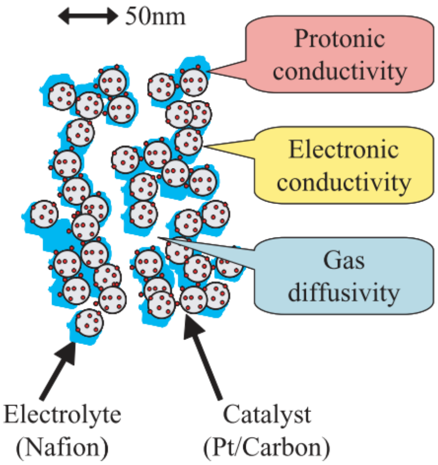

Figure 12 Schematic illustration of a catalyst layer
Source: Suzuki et al, Analysis of the Catalyst Layer of Polymer Electrolyte Fuel Cells [63].

On one hand, platinum is a rare metal and one of the most expensive metals on Earth. It is known for its allure in engagement rings, and because it works as an excellent catalyst, however the availability of this metal on Earth is limited. Without a cheaper substitute for platinum, these clean energy technology (PEMFC used in hydrogen vehicles) won’t be able to compete against means of transportation that burn fossil fuels [64].

On the other hand, the activated carbon is a common material used for supporting the Pt catalyst layers, thanks to its stability in both acid and basic media; in addition the fact that the carbon can be burnt off, allowing an economic and ecological effective recovery of the precious metal platinum[65]. Nowadays, there is a growing awareness of the need to study the surface chemistry of carbon-supported material to achieve an improvement on the catalyst performance. On way of modifying the catalytic behavior of activated carbon-supported noble metal catalysts can be done by increasing the active area through oxidation treatments of the support prior to metal loading [66].

1.2.3.2 Cost Analysis

A key factor that will determine the successful commercialization of the fuel cell technology is its cost competitiveness. Now, the predominant cost driver of a HFC vehicle is the amount of precious metal (Platinum) used on the PEMFC, that is the reason why researchers are striving to reduce the amount of Pt required for the cell by designing better materials [67]. As shown in **Figure 13**, the highest cost of FCV is on the fuel cell stack, contributing with a 41% of the overall system cost and if we go back to **Figure 6**, at the breakdown costs of fuel cell stacks, the catalyst is the most expensive component of the system.

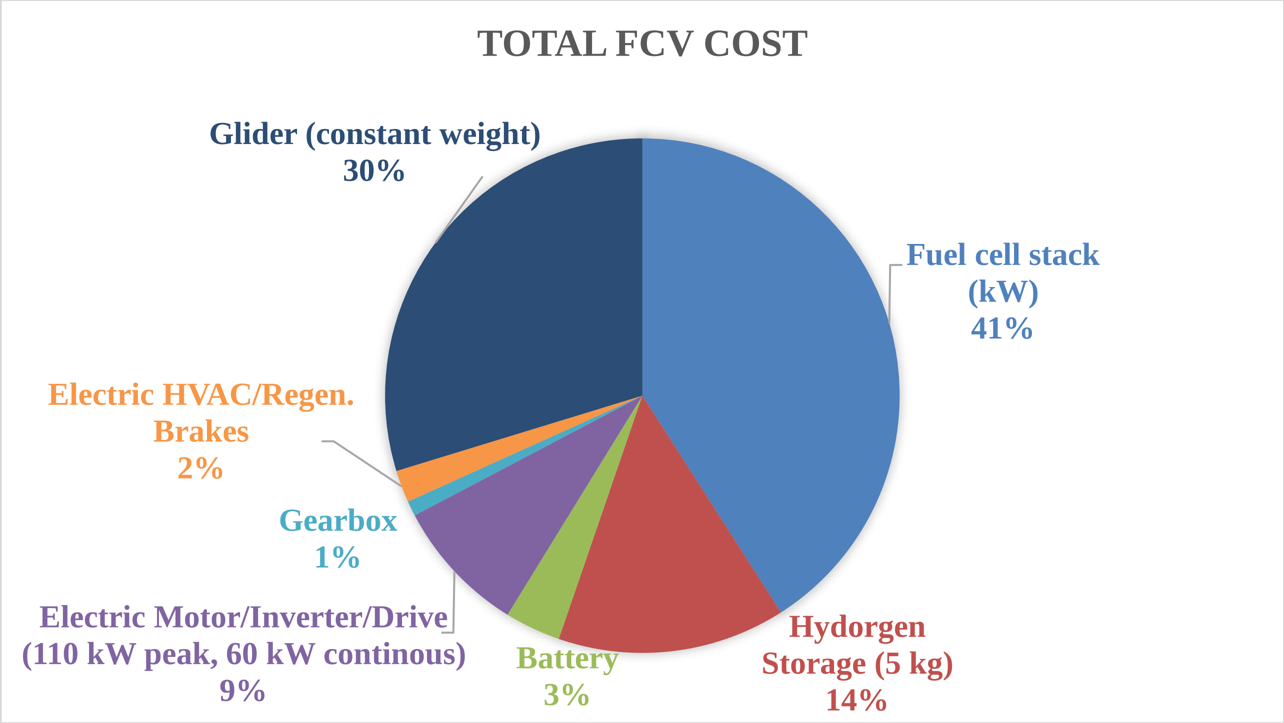

Figure 13 Estimates of breakdown FCV costs, 2016
Source: Own elaboration based on [51].

As previously mentioned, HFCEVs cannot be commercialize yet on a large scale because there is a significant technical-cost barrier, the high amount of Pt required on the CLs. Therefore, many research centers, universities, and government agencies are working on either reducing the platinum loading or developing non-platinum group metal catalysts (Hereafter PGM-free) [47].

1.2.3.3 Current Cost Optimization Methods

One of the problems on the objective of using less platinum as a catalyst is that these expensive catalyst is the most efficient alternative so it is important to make sure that the cheaper alternatives are not only less expensive but also at least as efficient [68]. Researchers at Stanford University have found a technique to increase the energy efficiency and performance of the platinum catalyst meaning it may be cost-effective in the end. Their developed method consists of a thin material (lithium cobalt oxide) that can strain a platinum lattice, both compressed and stretched out, and the catalytic activity is then doubled [69].

The design of electrodes of polymer fibers is a method that supports the catalyst because the surface area where reaction can occur is greater, which means that less Pt is needed. Scientists at the Vanderbilt University have found this fiber electrode design that also significantly boosts the fuel cell performance [70]. Another method of cost optimization is the development of non-precious metal catalyst, for example, researchers at the Washington State University have found a catalyst made of a nanomaterial called aerogel, consisting of about 92% air. That catalyst owns a high porosity that increases the surface area, therefore allows to reduce the need of Pt [71].

There are a lot of methods for cost optimization of PEMFC that are being discovered, research on-going in this field and improvements on electrodes and fuel cell catalysts are being done all the time. The improvements that have been described above are in an early stage of development; therefore, there is more work that needs to be done [72].

1.2.4 Performance and durability targets

The two primary metrics for analyzing the activity of a PGM catalyst are: specific activity (A/cm^2), and mass activity (A/mg_{PGM}) [73]. Due to the lingering kinetics of the oxygen reduction reaction, which is more less 5 orders of magnitude slower than hydrogen oxidation kinetics, the greater portion of the PGMs are required at the cathode side [74].

Researchers on PEMFC are aware of this challenge and focus their research on improving the catalysts used for the hydrogen oxidation at the cathode, as shown in the **Table 5**, the cathode has a higher Pt loading than the anode.

Case	**Anode Areal Loading mg_{PGM}/cm^2**	**Cathode Areal Loading mg_{PGM}/cm^2**	**Anode PGM Mass (g)**	**Cathode PGM Mass (g)**	**Normalized PGM Content g/kW (rated, gross)**
State-of-art	0.05	0.2	4.5	18	0.25
2020 DOE Target	0.025	0.1	2.3	9	0.125
Stretch Target	0.0125	0.05	1.1	4.5	0.0625

Table 5 Relationship between PGM real loading and absolute/Normalized Mass (90kW, $1W/cm^2$)
Source: A. Kongkanand and M. F. Mathias, The Priority and Challenge of High-Power Performance of Low-Platinum Proton-Exchange Membrane Fuel Cells [75].

Nonetheless, the reduction of Pt loading is expected to be reduce on both sides, anode and cathode, as shown in **Table 6**, the U.S. DOE had established performance and durability targets for the 2020 and in the long term, for the PGM-free and PGM cathodes used at the MEAs.

Characteristic	**Units**	**2015 Status**	**2020 Targets**
Platinum group metal total content (both electrodes)	g/kW (rated, gross) at 150 kPa (abs)	0.16	0.125
Platinum group metal (PGM) total loading (both electrodes)	mg_{PGM}/cm^2 (electrode area)	0.13	0.125
Mass activity	A/mg_{PGM} at 0.9 $V_{ir\text{-}free}$	>0.5	0.44
Loss in initial catalytic activity	% mass activity loss	66	<40
Loss in performance at 0.8 A/cm^2	mV	13	<30
Electro catalyst support stability	% mass activity loss	41	<40
Loss in performance at 1.5 A/cm^2	mV	65	<30
PGM-free catalyst activity	A/cm^2 at 0.9 $V_{ir\text{-}free}$	0.016	>0.044

Table 6 Technical targets: Electro catalysts for transportation applications
Source: Own elaboration based on [73][76][77][78][79].

1.2.5 Gas diffusion layers

The gas diffusion layers are the structural support of the CLs, and electrical conductors between the carbon supported catalyst and the current collector plates. The porosity, thickness, gas permeability and electric conductivity are important characteristics of the GDL that influence significantly on the performance of the fuel cells [80]. The GDLs with a graded porosity is beneficial for the electrode process of the cell reaction because large pores facilitate the transportation of liquid water generated, while the small pores are a gas difussion via that will enable the transport of gases that need to react [65].

1.2.5.1 Materials

GDLs are commercially available in various forms as carbon paper or woven carbon fabrics. Commonly the porous GDLs are made of a gas diffusion backing and a micro porous layer (MPL) [26]. The MPL is important for the enhancement of the cell performance and are usually made of carbon black powder and a hydrophobic agent like Polytetrafluoroethylene (PTFE). Even though the PTFE is not an electric conductor and high concentrations of it may reduce the electric conductivity of the GDL, the presence of PTFE is essential for proper water management [81].

1.3 Methods for reduction of platinum loading at the catalyst layers

During the past decade, researchers have being developing different catalyst with the objective of reducing the PGM present in the MEA and therefore reducing the production costs of the PEMFC technology. They had focused on the development promising ORR catalysts, because of its higher use of Pt [72]. These catalysts can be categorized as (1) Pt/C, (2) Pt and Pt alloy/de-alloy, (3) core-shell, (4) nonprecious metal catalysts (PGM-free), (5) shape-controlled Nano crystals, and (6) Nano frames, as shown in **Figure 14**, currently the catalyst used is the platinum catalyst supported by carbon particles (1), and the others (2, 3, 4, 5, 6) are being under development.

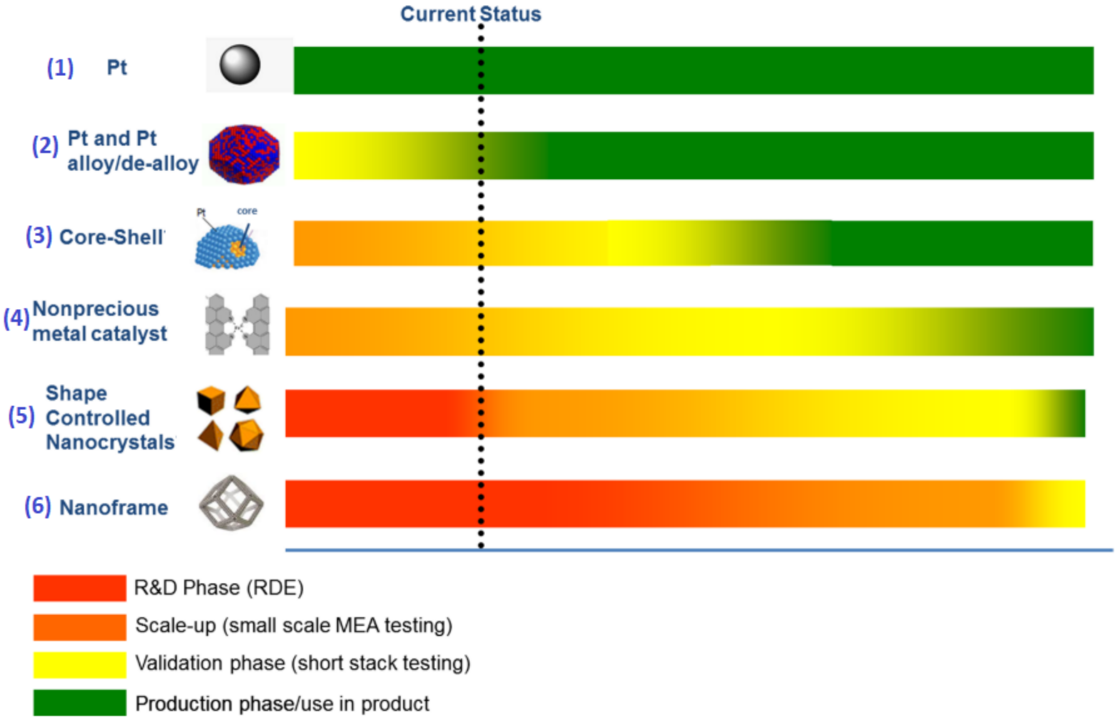

Figure 14 Development timelines for Pt, Pt alloy/de-alloy, core–shell, nonprecious metal, shape-controlled, and Nano frame ORR electro catalysts

Source: D. Banham and S. Ye, Current status and future development of catalyst materials and catalyst layers for proton exchange membrane fuel cells: An industrial perspective [82].

1.3.1 Direct reduction of Pt loading

The Pt/C is the simplest and most commonly type used as catalyst of PEMFC because when limiting the design of the catalyst to a single element, in this case platinum, there are no many options for improving the activity and durability of the cell. In fact, further improvements in activity and durability with conventional platinum supported by carbon catalyst rely on advances in “catalyst−support” interactions and modifications, nor in single material treatments [83].

The development of this Pt optimization method has reported enhancements on both activity and durability of PGM- based hydrogen oxidation at the cathode side. However, the several methods that follow this objective will not be able to meet long term mass activity requirements using conventional nanoparticles [84]. Nonetheless, if further PGM reduction is successfully achieved using this method(<6gPGM/vehicle), the cost of PGM itself will become a smaller fraction of the total fuel cell cost, making it unnecessary to entirely remove PGM [82].

1.3.2 Pt alloy electro catalyst

The second most developed method for reducing the platinum loading of the CLs are the Pt-alloys, like PtCo and PtNi catalysts. These materials are becoming the new baseline catalyst at the commercial level because they are able to achieve better durability than Pt/C while allowing high mass activities [85]. This almost mature optimization method has already been used on the catalyst layer of the Toyota Mirai, 2018 as shown in **Figure 15**.

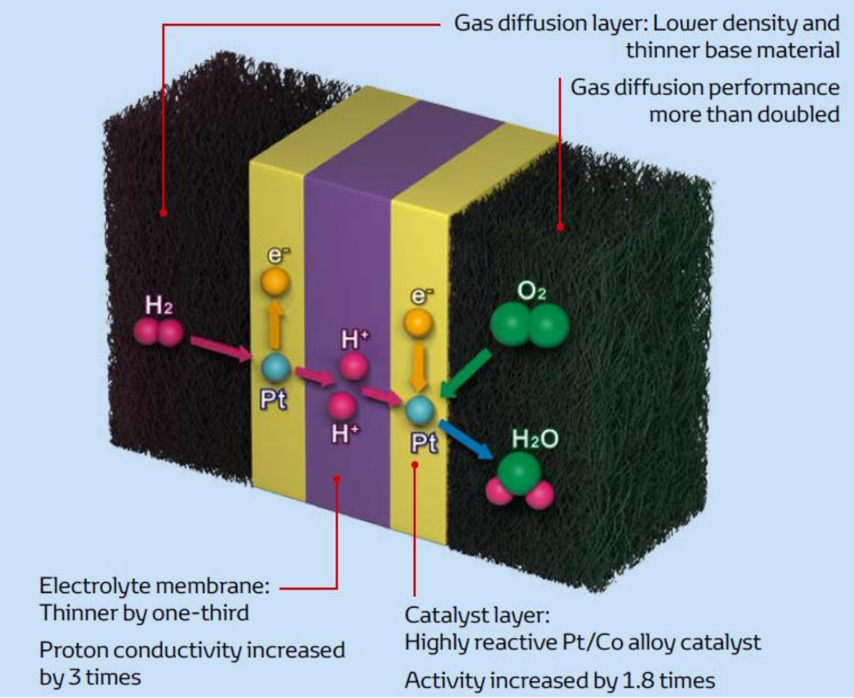

Figure 15 Electrode innovations Toyota Mirai, 2018
Source: S. T. Thompson *et al.*, Direct hydrogen fuel cell electric vehicle cost analysis: System and high-volume manufacturing description, validation, and outlook [16].

Carbon supported binary and ternary alloys have demonstrated up to three times higher mass activity than Pt/C, these improved electrocatalytic activity of Pt-alloys (Pt with other metals like cobalt, nickel, iron, titanium, aluminum, silver, among others) has been attributed to [26]:

- Smaller platinum bond distances.
- Structure sensitive inhibiting effect of OH ads.

Despite the high mass activity presented, improvements on the stability and durability of these catalysts have to be done. Further work on Pt-alloys has to be performed with the objective of removing the base metal poorly alloyed to the platinum [80].

There are some treatments that can be applied to the Pt-alloy by either acid and heat treatment, inhibiting a improved stability and activity, due to the formation of a richer platinum surface [87]. If these methods are further developed and proof a successful improvement on the durability of alloy catalysts, this type of catalyst could substitute the Pt/C at the MEA, and contribute to the cost optimization of PEMFC [82].

1.3.3 Core shell nanoparticles

During the past years, another type of material achieved an important progress; this is the core-shell nanoparticles, which is shown in **Figure 16**. This method relies on dispersing Pt particles only on the surface of the catalyst nanoparticle because this is the only active ORR catalyst, while another metal, like palladium, can make up the bulk optimizing the surface area of Pt. This method allows the highest possible platinum utilization, being an attractive cost effective method [88]. Perhaps the reduction of the cost achieved with this type of catalyst, on the cathode side is almost impossible to achieve to achieve PGM loadings <0.1 mg/cm2 with it [89].

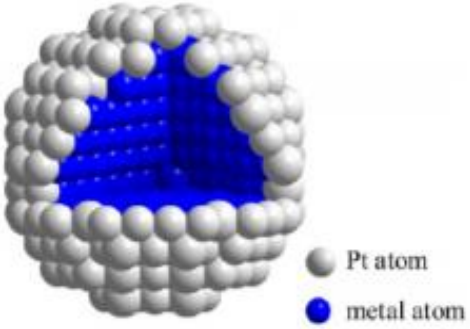

Figure 16 Basic concept of core−shell nanoparticles
Source: M. Oezaslan et al, Pt-Based Core−Shell Catalyst Architectures for Oxygen Fuel Cell Electrodes [90].

1.3.4 Shape Controlled Nano crystals (Pt-based nanoparticles)

There is another method similar to the core-shell nanoparticles called shape-controlled catalysts, where the structure of the particles are modified in a Nano scale, achieving a high specific activity by generating high mass activity with those nanostructure modifications [91]. At Georgia Institute of Technology, a group of researchers has developed a 9 nm $Pt_{2.5}Ni$ catalyst; despite the low Pt utilization afforded by the large 9 nm particles. In this study, a mass activity of 3.3 A/mg was achieved [92]. This achievement was accomplished through maintaining the ideal $Pt_{2.5}Ni$ crystal structure at a Nano scale; despite the great accomplishment still it has been obtain at a RDE level only, and more research has to be done so that it can be proved in industry [42].

1.3.5 Use of non-Pt group metals at CLs

As the ultimate goal on the development of PEMFC is to eliminate the PGM from the catalyst in order to reduce the production costs, there are some solutions with an approach of zero-Pt that are gaining attention. This approach consists of packing as many active sites as possible into a catalyst based on carbon and nitrogen, allowing a breakthrough in ORR activity [73]. However, non-PGM catalysts in the actual state of the art, are very unstable and this cause a poor performance at high power densities, due to mass transport limitations. This last aspect needs to be improved because it is required to provide acceptable ORR activity [75].

1.4 Low platinum loading PEMFCs

Despite there are been studied different methods, and novel materials for reducing the amount of platinum used on the CLs of the fuel cells and meet the targets established by the DOE; there are mature techniques that are been developed by research centers and industry that are capable of achieving low platinum loading PEMFCs. These techniques are mainly focused on the electrode fabrication method and the substrate and had achieved to increase the Pt utilization at the CLs while reducing the Pt-loading [93]. For example Su *et al.* developed a ultrasonic spray coating technique for low platinum loading proton exchange membrane fuel cell and achieved a loading on the cathode side of 0.350 mg/cm^2 [94]. There are other methods as thin film, electro deposition, sputter, brushing, bade coating; all of these differ on the way the electro catalyst is deposit on a substrate. However, these methods require more research for achieving a better performance of the cells while reducing more the amount of platinum deposited on the membrane [78].

A promising fabrication method of low platinum loading is the inkjet printing (Hereafter IJP) method that deposits the catalyst over the membrane. Methods such as spray deposition and screen-printing are not well suited for ultra-low Pt-loadings while the IJP method is very convenient for depositing small volume of catalyst diluted on a solvent mixture with a high precision thanks to the properties of a printing cartridge. In addition this method allow the uniform dispersion of the ink solution that contains the platinum particles supported by carbon black [95].

1.4.1 Challenges on the performance of low Pt-loading PEMFCs

The performance of a fuel cell can be characterize by the most common method of testing a fuel cell, a polarization curve. As shown in **Figure 17**, this curve is obtained by graphing the voltage output of the cell for a given current density and there can be clearly identified three distinct regions [96].

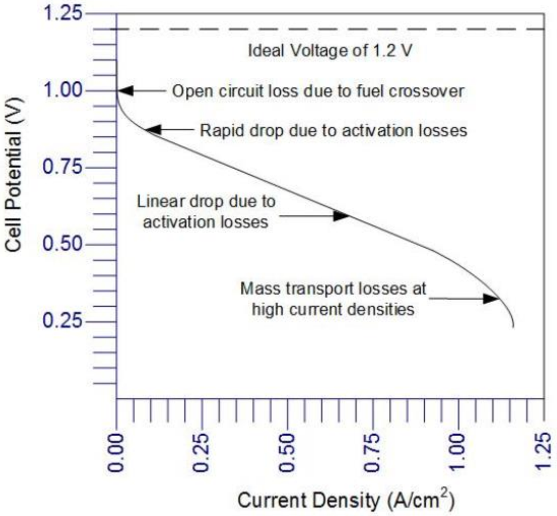

Figure 17 Typical polarization curve of a PEMFC
Source: C. Spiegel, Polarization Curves [96]

First, at low current densities the cell potential drops because of the activation losses. Second, at moderate current densities, the cell potential decreases more less linearly with current due to ohmic losses. Third at higher current densities, the cell potential drops in a more pronounced concentration losses also known as mass transport losses. Among these three potential losses, the most significant is the third one, however these mass transport losses can be reduced by finding an appropriate GDL [97].

As the fuel cell performance at high current densities is affected by mass transport losses due to water accumulation on the cathode side, a hydrophobic layer could be added to the catalyst layer to more effectively removal of the excess of water [98].

The excess of water also contributes to a rapid degradation of the membrane electrode assembly and a micro porous layer can enhance the performance of the ell by facilitating the liquid water transportation. More research has to be done in order to improve the performance of low platinum loading PEM fuel cells studying the effects of GDLs with different properties [24].

CHAPTER II

METHODOLOGY

In this chapter there will be described all the methods and procedures designed for the manufacturing, characterization, assembling and testing of PEM fuel cells, developed at the Energy Systems Design Laboratory at University of Alberta with the guidance of Dr. Marc Secanell, and the PhD candidate Manas Mandal.

As detailed on Chapter I: Theoretical Framework, the main components of the PEMFC are the membrane, catalyst layers (CLs), and the GDLs. The membrane as well as the GDLs were obtained from different suppliers, however the catalyst layers were fabricated preparing the catalyst ink (A) that was later deposited over the membrane using the inkjet printing method (B), see **Figure 18**. After fabricating the CLs, these were optically characterized using microscopes (C). Once the CLs were fabricate, these were assemble with different types of GDLs (D). Finally, the assembled PEMFCs were test on a fuel cell station (E), where different tests were conduct in order to study the performance of the cells. In the following paragraphs, there will be a detailed explanation of all the executed steps.

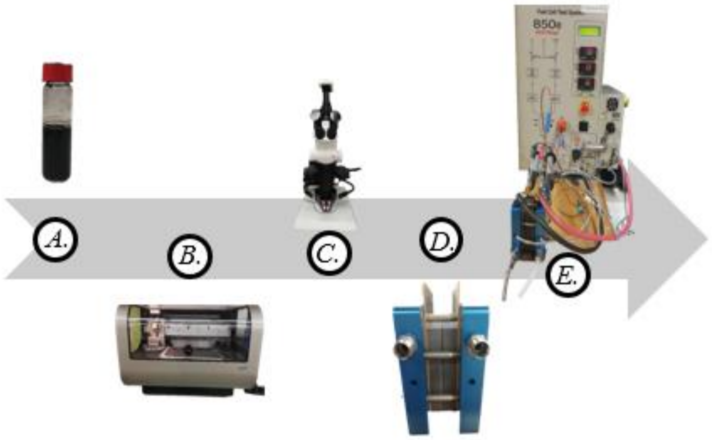

Figure 18 Experiments procedure
Own elaboration

3.1 Fuel cell fabrication

3.1.1 Ink fabrication

The first step for fabricating the fuel cell was preparing the ink that was going to be used for printing the catalyst layers. As mentioned on the introduction, the catalyst layers were compose mainly by platinum supported by carbon nanoparticles that enable a high surface area for the electrochemical reactions.

There are different commercial types of Pt/C powder, but for this study it was used the HyPlat platinum powder. This powder was dilute on a solvent mixture. Then this solution was place on a bath of sonication where was add the Liquion Nafion-solution. Finally, the solution was put on a probe sonicator device with a Micro-Tip for blending the whole mixture.

3.1.2 Inkjet printing

Once the ink was ready, it was injected on the cartridge of the Dimatix printer and the catalyst layers are printed over the Nafion membrane, where the printed area for each cell was 5cm^2. The inkjet printing method is the most simple and accurate method depositing the active catalyst electrode layer directly from print cartridges onto Nafion® polymer membranes. It allows deposition of materials in desired patterns without the need for complex processing and allowing the control the platinum loading. The tested cells were low-platinum loading because they operated with a minimum loading of Pt:

- Cathode: 0,1 mg/cm^2
- Anode: 0,005 mg/cm^2

For calculating the platinum loading, the following formula was use:

$$\text{Pt}_{\text{loading}} = \Delta\text{mass}_{\text{foil}} * \frac{\left(1 - \text{Nafion}_{\text{loading}}\right) * \left(\text{Catalyst Pt}_{\text{content}}\right)}{\text{Cell area}}$$

Once the desired amount of platinum was deposit over the membrane, the catalyst-coated membrane was dry overnight at atmospheric conditions, so that the remaining PG and IPA evaporate.

3.2 Fuel cell characterization

When the catalyst coated membrane (CCM) was already composed of platinum supported by carbon and Nafion, then the cathode and anode sides are characterized using an optical transmission microscope (Fisher microscope & Micron Program) and a stereoscopic microscope (Leica microscope and LAS program), respectively. These are qualitative methods for analyzing the microstructure of the CLs and see if they were properly print without cracks.

3.3 Fuel cell assembling

After the CCM was characterize, then it was ready for being assemble on a fuel cell. As the thickness of the GDLs that were used for this study varied, then gaskets with different thickness were needed. For calculating the thickness of the required gaskets the difference between the thickness of the gaskets and thickness of the GDL should have been 50 µm, see **Table *7***.

GDL type	GDL thickness	Gasket thickness
28BC	250 µm	200 µm
29BC	225 µm	170 µm
28BA	190 µm	140 µm
29BA	190 µm	140µm

Table 7 GDLs and gaskets thickness
Own elaboration

The different components of the cell were assembled based on **Figure 19** and the type of channels used for conducting the reactant gases were serpentine channels. A pressure test was done for verifying that the membrane electrode assembly was leak-proof using Pressurex sheets.

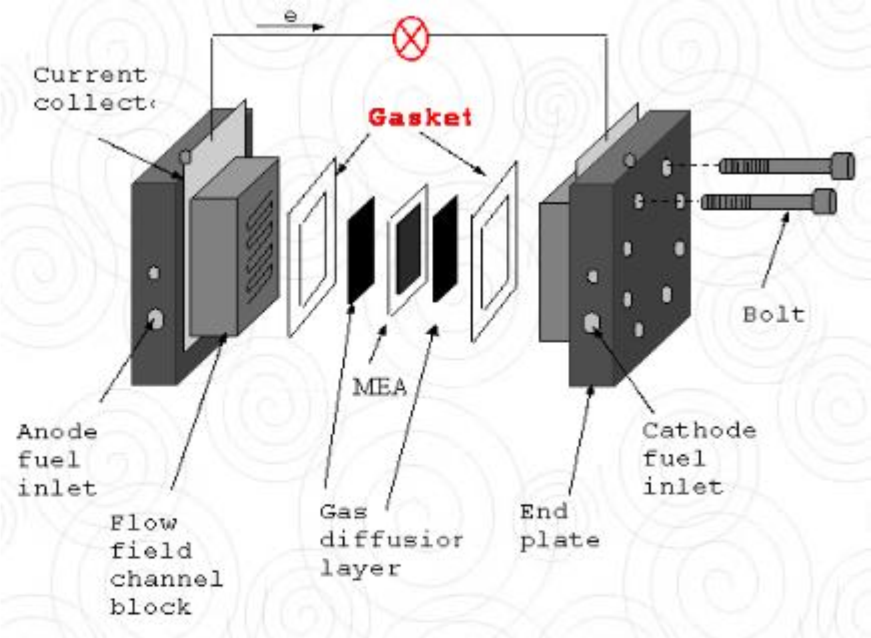

Figure 19 Assembling Setup
Source: NPTEL, Fuel Cell Technology [61]

3.4 Fuel cell testing

3.4.1 Testing station

The testing station used for this research is for single cell testing, therefore the performance results were only for each cell, the performance of a cell stack was not part of the scope of this work.

Every cell was first conditioned because the membrane needed to be hydrated so that it could perform effectively. This conditioning was perform at relative humidity of 80%, which means the anode and cathode sides operated at 74°C and the cell at 80°C. On the anode side it was applied a flow of 0.2 L/min and on the cathode side a flow of 0.4 L/min, using hydrogen and air as reactants, respectively.

After the conditioning, the cell was ready for being tested. The tests executed for studying the performance of the cells will be further explain in this chapter.

3.4.2 Tests executed

Polarization Curves

The first tests that were perform were polarization curves, at different humidity levels. The station parameters are show in **Table 8**.

Test Station Parameters	**Value**	
Cell temperature	60 °C	80 °C
Anode relative humidity	90 %	50/70/90 %
Cathode relative humidity	90 %	50/70/90 %
Anode flow rate (H_2)	0.1 slpm	0.1 slpm
Cathode flow rate (Air)	0.1 slpm	0.1 slpm
Wet stoichiometry	2/6	2/6
Back pressure	50 kPa	50 kPa

Table 8 Polarization curves test station parameters
Source: Own elaboration

The polarization curves plot the cell voltage against the current density showing the general performance of the cell. With these tests, the irreversible losses can be identify as the following: Kinetic activation resistance on the first drop, ohmic resistance on the second drop and mass transport resistance on the third drop. These tests were perform at the Fuel Cell Station with the potentiostat and backpressure system.

Cyclic Voltammetry

The other performed test was the cyclic voltammetry, which is a common diagnostic tool for characterizing the catalyst layer. It allows to experimentally determine the electrochemical surface area (ECSA), which is the active area of platinum that is involve on the electrochemical reaction.

This test was perform at 30°C and 80°C and the cathode was purged with an inert gas, nitrogen while the anode was fed with hydrogen, the test parameters are shown at **Table 9** and equipment used for them was the Fuel Cell Software and the BioLogic Potentiostat.

Test station parameters	Value	
Cell temperature	30	80
Anode temperature	28	77
Cathode temperature	28	77
Cathode flow rate (N_2)	0.005 slpm	0.005 slpm
Anode flow rate (H_2)	0.2 slpm	0.2 slpm

Table 9 Cyclic voltammetry test station parameters
Source: Own elaboration

In order to calculate the ECSA, a code developed in Python by Michal Moore for the ESDLab was use for processing the data, as shown in **Figure 20**, the graph on the right side is a typical cyclic voltammogram, and the colored green area is the ECSA.

Platinum loading (mg/cm^2): 0.1008
Cycles to skip (-): 5.0
Area of the fuel cell (cm^2): 5.0
Number of cycle (-): 10
Scanrate (V): 0.04

```
== Welcome to the ESDLab CyclicVoltammetry program ==

Introduction
============
This program can read in CV data from the Scribner potentiostat (in the form of .fcd files) and calculate parameters
such as the ECSA, double layer capacitance and crossover. As an overview, the code will read in the measured
potentials and currents, separate the data into different cycles and find an average of the cycles. This averaged CV is
then used to find the double layer by finding the minimum and maximum current between 0.3V and 0.6V. The ESCA can
then be found by integrating under the CV curve to the double layer, between potentials of 0.1V and 0.4V. The former
removes the hydrogen evolution peak, while the later is the extent of the hydrogen ion adsorption region. An image
should be shown showing the CV and the results from the simulation will be displayed in the results text box.

Setting up the simulation
=========================
Ideally this code is run from terminal or from Spyder. If running from Spyder, set it up to run in an external console.
With the run.py being displayed, click Run>Configuration per file...>Execute in an external system terminal
The advantage of running in this mode is that the CV graph will be displayed in an external window which can be
manipulated.

1. Load a file by clicking File>Load. Files can be in the form of .fcd, .par or .txt
2. Some information will be displayed in the terminal window, check for errors
3. Depending on the type of file being loaded, some information can now be inputted to the simulation through the
GUI. Ensure that the relevant data is entered. Note that 'Cycles to skip' will remove cycles from the start of the
dataset.
4. Choose whether to calculate the upper or lower area using the Area menu option. Ideally both should give the same
answer.
5. The limits for the integration are chosen using the Limits menu. The default option is to use 0.1V and 0.4V, manual
will allow the user to input the limits and automatic means that the code will attempt to find the leftmost limit by looking
at the slope of the lower peak near 0.1V. This method is not particularly accurate, so a graph showing the CV and the
proposed location of the limit will be displayed. In the terminal window, set the desired limit and hit enter.
```

```
5.172851041666666483e-02    -1.546364687500000201e+01
5.172414583333333205e-02    -1.508065625000000054e+01
5.171978124999999926e-02    -1.469766562500000084e+01
5.171541666666666648e-02    -1.431467500000000115e+01
5.171105208333333370e-02    -1.393168437500000145e+01
5.170668750000000091e-02    -1.354869375000000176e+01
5.170232291666666813e-02    -1.316570312500000206e+01
5.169795833333333535e-02    -1.278271250000000236e+01
5.169359375000000256e-02    -1.239972187500000267e+01
5.168922916666666978e-02    -1.201673125000000297e+01
5.168486458333333700e-02    -1.163374062500000150e+01
5.168050000000000421e-02    -1.125075000000000180e+01
5.167613541666667143e-02    -1.086775937500000211e+01
5.167177083333333865e-02    -1.048476875000000064e+01
5.166740625000000586e-02    -1.010177812500000094e+01
5.166304166666667308e-02    -9.718787500000001245e+00
5.165867708333334030e-02    -9.335796875000001549e+00
5.165431250000000751e-02    -8.952806250000001853e+00
5.164994791666667473e-02    -8.569815625000002157e+00
5.164558333333333501e-02    -8.186825000000002461e+00
5.164121874999999529e-02    -7.803834375000002765e+00
5.163685416666666250e-02    -7.420843750000002181e+00
5.163248958333332972e-02    -7.037853125000001597e+00
5.162812499999999694e-02    -6.654862500000001901e+00
5.162376041666666415e-02    -6.271871875000002206e+00
5.161939583333333137e-02    -5.888881250000001621e+00
5.161503124999999859e-02    -5.505890625000001037e+00
5.161066666666666580e-02    -5.122900000000001342e+00
```

```
IndexError: index -1 is out of bounds for axis 1 with size 0

Traceback (most recent call last):

  File "C:\Users\ezquerra\Desktop\Elena Ezquerra\repo\electrochemicalmethods\CyclicVoltammetry\source\
    results = myEq.solve(paramsDict, ManualInputWindow)

  File "C:\Users\ezquerra\Desktop\Elena Ezquerra\repo\electrochemicalmethods\CyclicVoltammetry\source\
    averagefunction(initParams)

  File "C:\Users\ezquerra\Desktop\Elena Ezquerra\repo\electrochemicalmethods\CyclicVoltammetry\source\
    initParams['sortpot'][:,-1] = np.nanmean(initParams['sortpot'][:,int(initParams['skip']):-1], axis

IndexError: index -1 is out of bounds for axis 1 with size 0

All important data like Vmin, Vmax, scanrate were imported from the *.fcd file

One cycle has around 575 values
Number of cycles: 10
Load a File
```

```
All important data like Vmin, Vmax, scanrate were imported from the *.fcd file

One cycle has around 575 values
Number of cycles: 0
Load a File
Traceback (most recent call last):
```

Figure 20 Cyclic voltammetry test.
Source: Own elaboration

Limiting Current

The general implication of the limiting current condition is that the reaction rate at the cathode is limited by how quickly oxygen diffuses to the electrode's surface. The total oxygen transport resistance R_{total} can be calculated at limiting current, using the following formula:

$$R_{total} = \frac{4F c_{O2}}{i_{lim}}$$

Where c_{O2} is the gas channel oxygen concentration, i_{lim} is the measured limiting current density and F is the Faraday constant.

The limiting current experiment is conducted with H_2 on the anode and 1% oxygen in nitrogen on the cathode side. The voltage is scanned as at a polarization curve, but only the las part of the graph is of interest. On **Table 10** are the station parameters for the test and on **Figure 21** is a common graph of a limiting current experiment of PEMFC.

Test station parameters	**Value**
Cell temperature	80
Anode temperature	72
Cathode temperature	72
Cathode flow rate (N_2)	0.2 slpm
Anode flow rate (H_2)	2 slpm
Back pressure	0 kPa

Table 10 Limiting current test station parameters
Source: Own elaboration

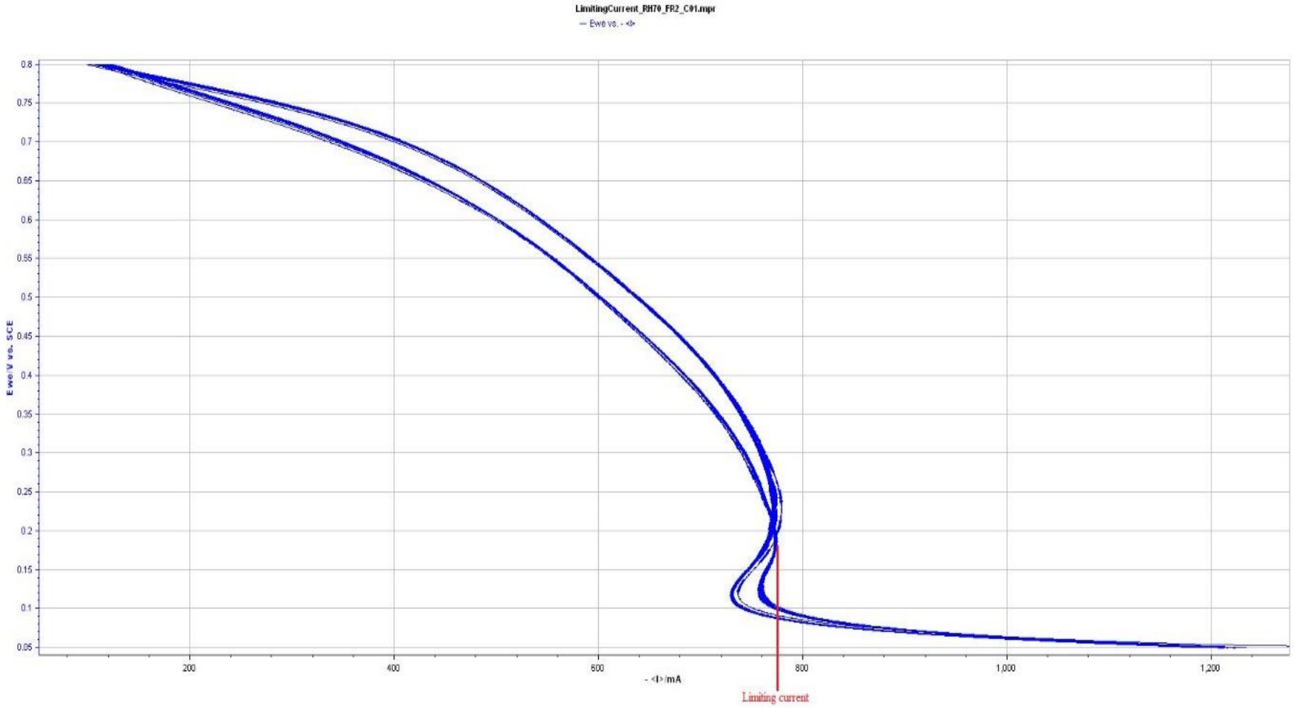

Figure 21 Limiting current test graph
Source: Own elaboration based on experimental data and the program EC-Lab V11.21

3.4.3 Reproducible data

In order to guarantee that the process of fabrication, assembling and testing were done properly and that the obtained data was reliable, first two batch of four cells each were fabricated, assembled and tested under the exact same conditions until at least three cells presented reproducible results. The results of the repeatable data can be verified on the polarization curves (see **Annex *7***) and the cyclic voltammograms obtained (see **Annex *8***).

CHAPTER III

RESULTS

This thesis is based on experimental research conducted at the Energy Systems Design Laboratory. The results that will be presented on this chapter were obtained following the methodology previously explained. For obtaining reliable results, first a standard process of fuel cell fabrication, characterization, assembling and testing was done in order to learn the techniques, and two batch of four cells each were fabricated until obtaining reproducible data. Once the repeatability was achieved, then the experiments subject of this thesis were conducted. This whole process took 4 months.

3.1 Fuel cell fabrication

3.1.1 Ink fabrication

The components of the ink for fabricating the CCM remained always the same as well as the quantities for printing one batch of four cells; these constituents are in detail at the **Table 11** and on **Figure 22** is showed a 3 mL sample of the ink.

Component	Type
Platinum catalyst supported by carbon	HyPlat 40wt%
Solvent mixture	Propylene glycol (PG)
	Isopropylene alcohol (IPA)
Ionomer solution	Liquion 5wt% Nafion

Table 11 Constituents of the ink
Source: Own elaboration

Figure 22 3 mL sample of ink
Source: Own elaboration

3.1.2 Inkjet printing

In total, four batches of cells were printed, the first two were for obtaining reproducible data with the standard process, and the other two were for testing the different GDLs. The platinum loading obtained after printing was the same for all the batches. At the cathode side, it was always obtained a final loading of 0,1008 $\mathrm{mg/cm^2}$ after printing 11 layers, whereas at the anode side, it was obtained a final loading of 0,0504 $\mathrm{mg/cm^2}$ after printing 6 layers. These values were calculated after the CCMs dried overnight. **Figure 23** shows a batch of cells with the anode and cathode side printed.

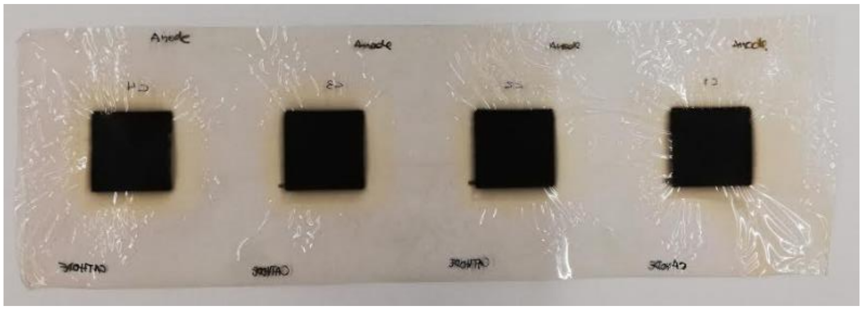

Figure 23 Batch of CCMs
Source: Own elaboration

3.2 Fuel cell characterization

In order to characterize the structure of the printed CCMs, they were observed using microscopes. The first two batches of printed cells were for obtaining reproducible data, therefore for the fabrication of those CCMs it was followed the standard process, however when characterizing the cells it was observed the presence of many cracks, as it can be seen in **¡Error! No se encuentra el origen de la referencia.**.

After reading different studies about the factors that influence the generation of cracks on nanostructures of platinum catalyst supported by carbon, Kumano *et al*. explained that the cracks are generated when the solvent breaks through the catalyst structure for evaporating [99]. Based on this, during the printing process, it was established a drying time for allowing the solvent to evaporate little by little between layers and on **Table 12**, it can be seen clearly how the number of cracks decreased with 90 seconds of drying between layers. This change was applied for the CCMs that were used for testing the different GDLs.

Component	**Resolution**	**Without drying time between layers**	**With 90 seconds of drying between layers**
Cathode	1 mm	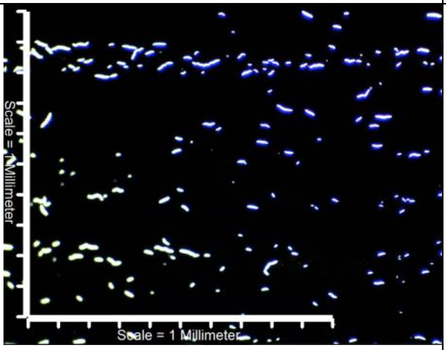	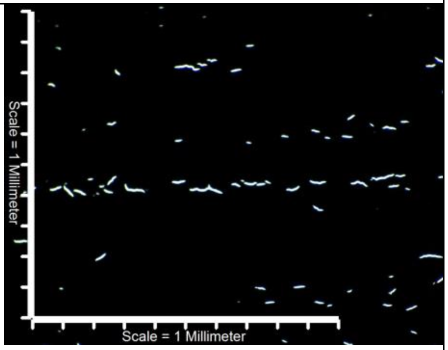
	2 mm	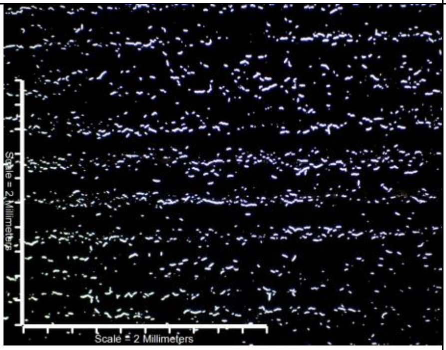	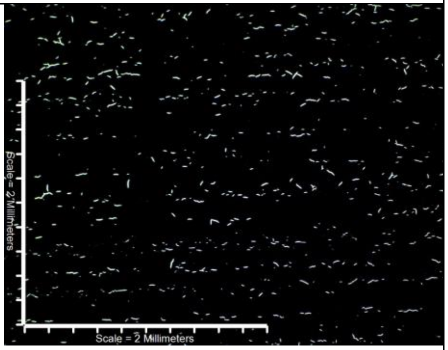
Anode	1 mm	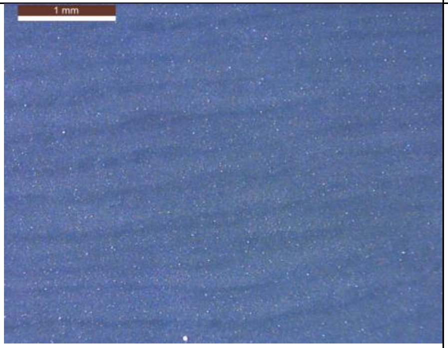	
	200 µm		

Table 12 Optical characterization of CCMs
Source: Own elaboration

3.3 Fuel cell assembling

The fuel assembling was done with different GDLs; therefore, gaskets with different thickness were used. Because of it, the pressure tests shown on **Table 13** look different between each type of GDL, however all of them show serpentine channels, which is the reason why it was concluded that the assembly was correct, that there was not going to occur any leaking of gases and that the experiments at the fuel cell station can be done.

GDL		**Pressure test**
28 BC	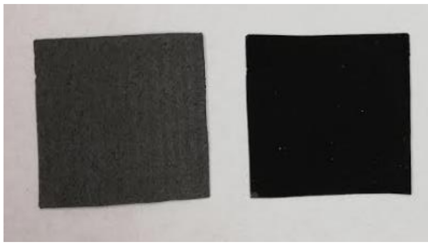	
29 BC	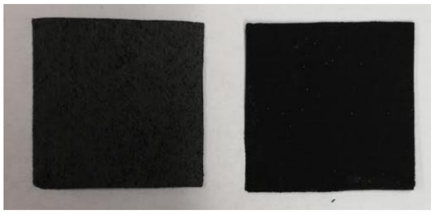	
28 BA	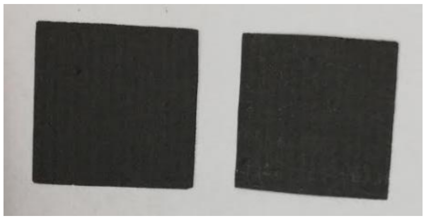	
29 BA	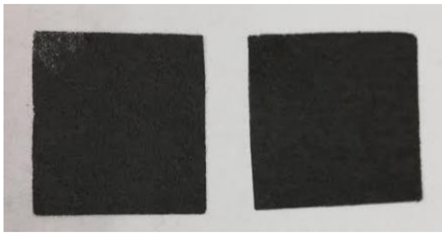	

Table 13 Pressure tests
Source: Own elaboration

3.4 Fuel cell testing

In order to obtain reliable results, two batch of cells were fabricated and tested following the exact same procedure. Therefore, in the following sections there will be showed the results obtained from the tests executed with those two batch of four cells each, giving repeatable trends on the performance of the cells with the four different GDLs (28BC, 29BC, 28BA and 29BA). For facilitating the order and comprehension of the results, they will be identified by the roman number I for the first batch of tested cells, and by the roman number II for the second batch.

3.4.1 Tests executed

Polarization Curves

As explained on the previous chapter, polarization curves allow identifying the major losses during the operation of a fuel cell. **Figure 24** shows the polarization curves obtained with four different GDLs at different levels of relative humidity (50, 70 and 90%). With this test, it can be also obtained the cell resistance by plotting the E_iR_Avg in function of the current densities, these graphs are shown in **Annex 9**, **Annex 10**, and **Annex 11**.

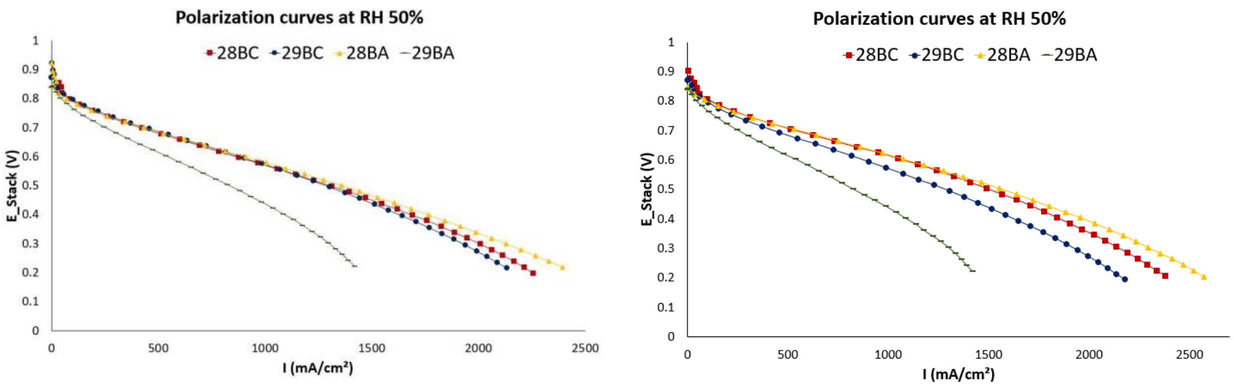

I

II

(a)

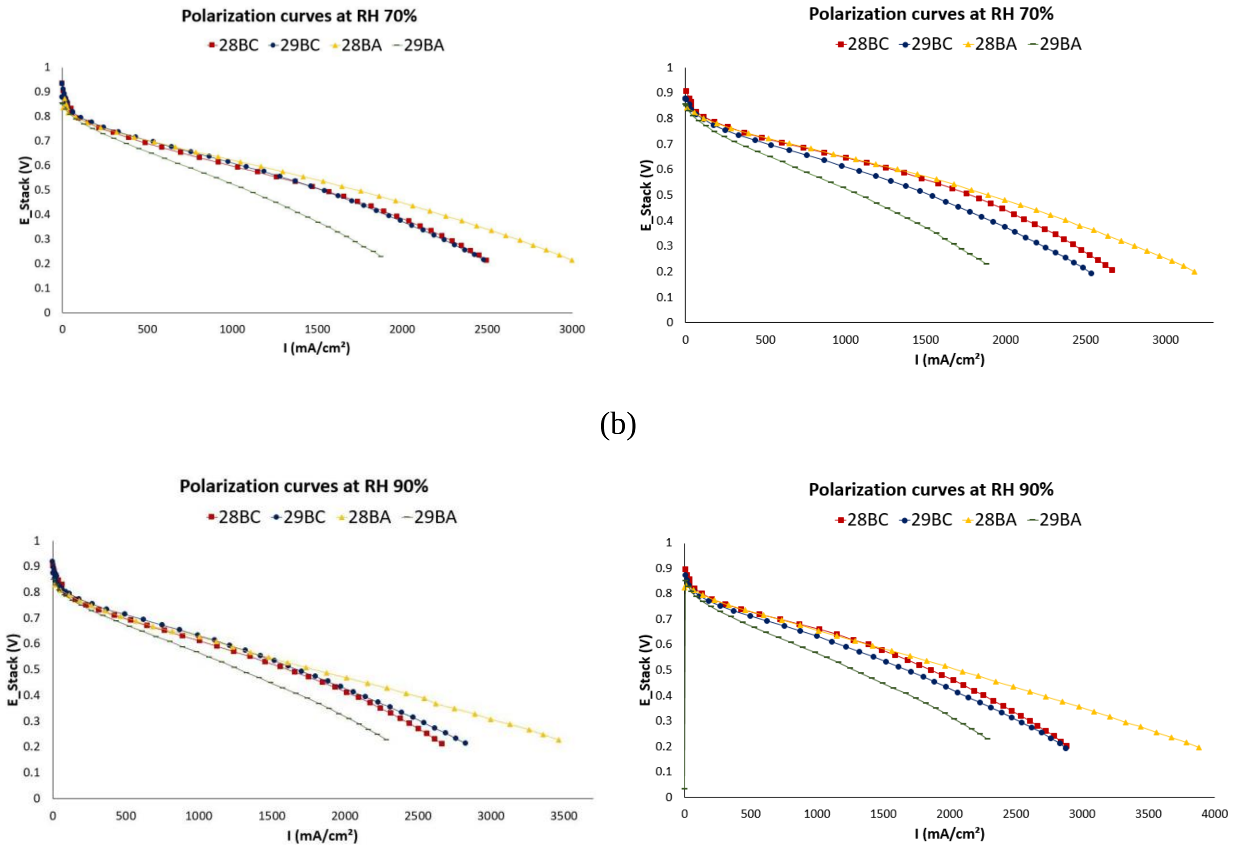

(b)

(c)

Figure 24 Polarization curves with different GDLs and at different relative humidity (a) 50% (b) 70% (c) 90%
Source: Own elaboration using the data from the FC Software

Cyclic Voltammetry

The cyclic voltammetry test is a tool for identifying if there is a crossover or short circuit during the fuel cell operation and for calculating the electrochemical surface area. **Figure 25** depicts the cyclic voltammograms obtained from the fuel cell station after testing the cells with the four different GDLs.

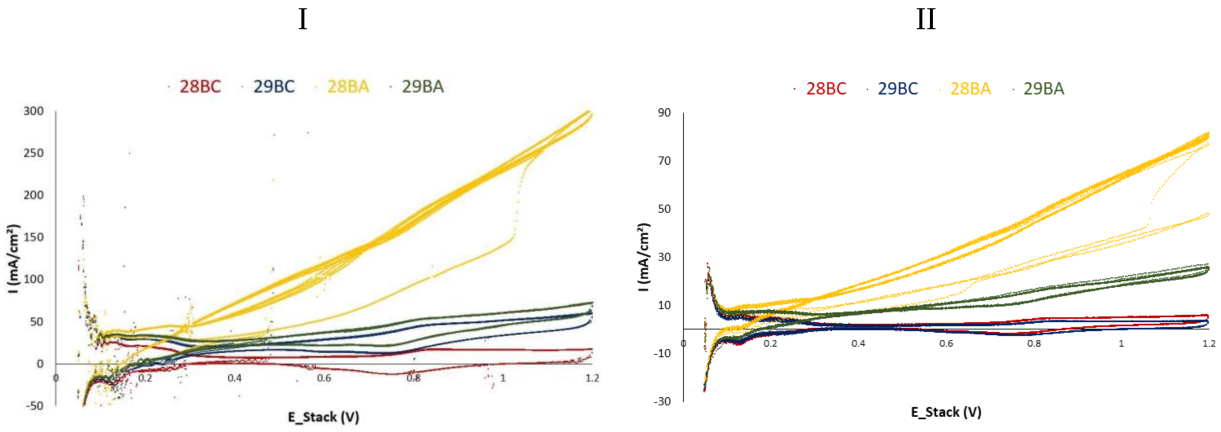

Figure 25 Cyclic voltammogram at 30°C with different GDLs
Source: Own elaboration using the data from the FC Software

As it can be observed, the cell with the 28BA GDL presents a short circuit represented as a huge crossover at the cyclic voltammogram. The other three cells show a regular CV, however the cell with the 29BA GDL shows a higher crossover than the BC series because the carbon fibers intrudes into the CCM generating electron conductivity through the membrane and this does not happen with the BC series because of the presence of a MPL on the 28BC and 29BC GDLs.

Limiting Current

The limiting current experiments were conducted with the BioLogic Software. This test graphs a polarization curve with an excess of oxygen and from the graphs obtained with different GDLs (see **Annex 12**, **Annex 13**, **Annex 14**, and **Annex 15**). From these graphs there could be obtained the limiting currents for the different GDLs tested, whose average values are shown on **Table 14**.

Cell	Average of limiting current
28BC	732 mA
29BC	895 mA
28BA	966 mA
29BA	1430 mA

Table 14 Limiting currents for the cells with different GDLs
Source: Own elaboration

As it can be seen from **Table 14**, the BA GDLs have a higher limiting current therefore a lower mass transport resistance than the BC GDLs. This can be explain by the presence of bigger pores in the macrostructure of the BAs through were the water is evacuated, avoiding the flooding of the cell at high current densities. The BCs have an extra layer (the MPL), therefore the structure of this type of GDLs has more pores of smaller sizes reducing the area through which the water could be evacuated.

CONCLUSIONS

In the last decades, it has been proved the benefits that the technology of fuel cells has for the environment and the energy sector. The applications of hydrogen fuel cells range from industrial backup power systems to means of transport like light duty vehicles, buses, trains and heavy-duty trucks. However, this technology still cannot be massively implemented mainly because of one hurdle, the high manufacturing costs.

Researchers and developers have identified the use of platinum on the catalyst area of the fuel cell as the major cost of this technology. In order to promote the large-scale commercialization of the fuel cell technology and ensure the transition to a clean transport sector, catalyst developments need to be done. The development of Pt catalyst supported by carbon is the most advanced method for Pt reduction however it is still needed to improve durability and performance through innovative catalyst layer designs that can be modified by different fabrication techniques.

In this thesis it was studied the performance of low platinum loading PEM fuel cells that were fabricated using the inkjet printing method and assembled with four different types of SIGRACET® GDLs (28 BC, 29BC, 28 BA and 29BA). The performance was studied based on the results obtained from the polarization curves, cyclic voltammetry and limiting current tests. After testing the first batch of cells under standard conditions, the major losses were identified on the mass transport region, and after performing a literature of review about the problems on the operation of low Pt-loading PEMFC, the water management was identified as the major problem. However, literature states that the addition of MPLs on the GDLs is the main solution to the water management problem.

In order to study the effects of the different properties of GDLs, like porosity, carbon matrix, and presence of a MPL, on the performance of low Pt-loading PEMFC; various cells were fabricated using the inkjet printing method and were assembled and tested with different SIGRACET® GDLs. The conclusions of the study of the effects of different SIGRACET® GDLs on the performance of PEMFC are the following:

1. There is no significant difference between the performance of the cells with the GDLs 28BC and 29BC; therefore, it can be conclude that the MPL is predominant when comparing the performance of the cells with GDLs with different pore size distribution (see **Annex *16*** and **Annex *17***). The BC series gives a better performance than the 29 BA, and does not have a crossover problem as the BA series because the MPL has a better contact with the CLs, avoiding the intrusion of the carbon fibers into the CCM.
2. In theory, the GDL with MPL (BC series) should give the best performance, however the 28BA showed an outstanding performance reaching up to 4 A/cm^2 at wet conditions. This could be explained by the pore size distribution obtained by the PhD candidate Fei Wei from the ESDLab (see **Annex *16*** and **Annex *17***); with a higher number of big pores, the excess of water generated at high current densities can be easily evacuated through those pores. Therefore, the GDL that gives the best performance is the 28 BA even the cross over problem, but until this problem is solved, it is recommend using the 28 BC because it gives a good performance and has not this problem.
3. Given the cyclic voltammograms, it can be concluded that there is a short circuit with the BA series. The only reason for explaining a short circuit is a hole through the membrane, and this could be because of the carbon fiber intruding into the CLs.

As future work, some steps from the methodology could be optimized. First, the drying time between layers during the inkjet printing process can be further explored at a wider range of time; and the effects of them on the performance of the cells should be studied. Second, in order to determine with certainty if there are holes through the membrane after testing the cell, a new set up could be built for characterizing the cells after each test and reduce the uncertainty about the presence of holes. Finally, the inkjet printing method could be applied for printing MPLs over the catalyst layers and study the effects of it on the performance of the cell at high current densities.

REFERENCES

[1] H. Kargupta, J. Gama, and W. Fan, “The next generation of transportation systems, greenhouse emissions, and data mining,” *Kdd*, pp. 1209–1212, 2010.

[2] “United Nations Framework Convention on Climate Change. Kyoto protocol: Status of ratification,” 2009.

[3] J. Watts and J. Watts, “Domino-effect of climate events could move Earth into a ‘hothouse’ state,” *Guard.*, 2018.

[4] J. Vidal and A. Vaughan, “Paris climate agreement ‘may signal end of fossil fuel era,’” Dec. 2015.

[5] J. G. J. Olivier, K. M. Schure, and J. A. H. W. Peters, “Trends in global CO2 and total greenhouse gas emissions,” 2017.

[6] M. F. Felgenhauer, “Battery and fuel cell electric vehicles in the context of the energy transition,” 2016.

[7] Eurostat, “Greenhouse gas emission statistics-emission inventories,” 2018.

[8] EPA, “U.S. Transportation Sector Greenhouse Gas Emissions, 1990-2016,” 2018.

[9] “International Energy Agency, CO2 emissions from fuel combustion,” 2018.

[10] *Transitions to Alternative Transportation Technologies--A Focus on Hydrogen*. National Academies Press, 2008.

[11] C. E. Thomas, “Fuel cell and battery electric vehicles compared,” *Int. J. Hydrogen Energy*, vol. 34, no. 15, pp. 6005–6020, Aug. 2009.

[12] G. Van De Kaa, D. Scholten, J. Rezaei, and C. Milchram, “The battle between battery and fuel cell powered electric vehicles: A BWM approach,” *Energies*, vol. 10, no. 11, 2017.

[13] G. J. Offer, D. Howey, M. Contestabile, R. Clague, and N. P. Brandon,

"Comparative analysis of battery electric, hydrogen fuel cell and hybrid vehicles in a future sustainable road transport system," *Energy Policy*, vol. 38, no. 1, pp. 24–29, Jan. 2010.

[14] J. Shang, "THE ROLE OF HYDROGEN AND FUEL CELLS FOR ULTRA LOW CARBON VEHICLES," 2014.

[15] J. L. Shang and B. G. Pollet, "Hydrogen fuel cell hybrid scooter (HFCHS) with plug-in features on Birmingham campus," *Int. J. Hydrogen Energy*, vol. 35, no. 23, pp. 12709–12715, Dec. 2010.

[16] S. T. Thompson *et al.*, "Direct hydrogen fuel cell electric vehicle cost analysis: System and high-volume manufacturing description, validation, and outlook," *J. Power Sources*, vol. 399, no. August, pp. 304–313, 2018.

[17] "International Energy Agency, Towards cross-modal electrification," 2018.

[18] "Union of Concerned Scientists, Accelerating US Leadership in Electric Vehicles," 2017.

[19] S. M. Knupfer, R. Hensley, P. Hertzke, P. Schaufuss, N. Laverty, and N. Kramer, "Electrifying insights: How automakers can drive electrified vehicle sales and profitability," 2017.

[20] E. Viable *et al.*, "Hydrogen Fuel Cells for Transportation," vol. 6, p. 68, 2018.

[21] J. B. Gaillard and G. Kleen, "PGM Free Catalysts for PEMFC - DOE Hydrogen and Fuel Cells Program FY 2015 Annual Progress Report," 2015.

[22] *Cost, Effectiveness, and Deployment of Fuel Economy Technologies for Light-Duty Vehicles*. The National Academies Press, 2015.

[23] A. Vehicles, B. Energy, E. Systems, D. Engineering, and P. Sciences, *Transitions to Alternative Vehicles and Fuels*. National Academies Press, 2013.

[24] S. Shukla, J. Zhou, M. S. Saha, M. Tam, J. Stumper, and M. Secanell, "Inkjet Printed Electrode Coated Membrane with Ionomer Based Carbon Micro-porous Layer."

[25] W. K. Lee, C. H. Ho, J. W. Van Zee, and M. Murthy, “Effects of compression and gas diffusion layers on the performance of a PEM fuel cell,” *J. Power Sources,* 1999.

[26] M. H. Shojaeefard, G. R. Molaeimanesh, M. Nazemian, and M. R. Moqaddari, “A review on microstructure reconstruction of PEM fuel cells porous electrodes for pore scale simulation,” *Int. J. Hydrogen Energy,* vol. 41, no. 44, pp. 20276–20293, 2016.

[27] J. Jeevarajan, “Cells and Batteries,” pp. 387–407, 2014.

[28] T. Koppel and J. Reynolds, “A Fuel Cell Primer,” 2001.

[29] B. Cook, “An introduction to fuel cells and hydrogen technology,” 2001.

[30] “FUEL CELL BASICS 1. Origins and principle.”

[31] B. Y. W. F. Podolski, T. G. Benjamin, and J. P. Kopasz, “Fuel cells 11.9.”

[32] “Fuel Cell Handbook (Seventh Edition),” 2004.

[33] U. Environmental Protection Agency, C. Heat, and P. Partnership, “Catalog of CHP Technologies, Section 6. Technology Characterization – Fuel Cells,” 2015.

[34] “Fuel cell basics-Technology types,” 2012. [Online]. Available: www.fuelcelltoday.com. [Accessed: 29-Nov-2018].

[35] L. Giorgi and F. Leccese, “Fuel Cells: Technologies and Applications,” *Open Fuel Cells J.,* vol. 6, pp. 1–20, 2013.

[36] “FUEL CELL ENGINE TECHNOLOGY,” 2010.

[37] B. Sorensen, “Electrochemical Energy Conversion,” *Renew. Energy,* vol. 9, pp. 488–495, 2011.

[38] J. M. Nail, G. Anderson, G. Ceasar, and C. J. Hansen, “The Evolution of the PEM Stationary Fuel Cell in the U.S. Innovation System.”

[39] A. Schmitz, “Principles of General Chemistry,” 2012.

[40] G. E. Haslam, J. Jupesta, and G. Parayil, “An Analysis of Fuel Cell Technology for Sustainable Transport in Asia,” no. 1999, pp. 1–12, 2010.

[41] J. Blanchard, "Smart Energy Solutions Using Fuel Cells."

[42] US Office of energy efficiency & renewable energy, "Fuel Cells," *Fuel Cell Technol. Off. Multi-Year Res. Dev. Demonstr. Plan*, vol. 2015, p. 3.4.1-3.4.58, 2017.

[43] S. Sevencan, *Economic Aspects of Fuel Cell-Based Stationary Energy Systems*. .

[44] K. V. Kordesch and G. R. Simader, "Fuel Cells," 1996.

[45] "Fuel Cells," *Fuel Cell Technol. Off. Multi-Year Res. Dev. Demonstr. Plan*, vol. 2015, no. 3.4, pp. 1–58, 2016.

[46] "FUEL CELL TECHNOLOGIES, Energy Efficiency & Renewable Energy (U.S. Department of Energy)," 2010.

[47] B. D. James, J. M. Huya-Kouadio, C. Houchins, D. A. Desantis, D. Manager, and A. Wilson, "Fuel Cell Vehicle Cost Analysis; DOE Hydrogen and Fuel Cells Program FY 2017 Annual Progress Report," 2017.

[48] J. Garche and L. Jörissen, "Applications of Fuel Cell Technology: Status and Perspectives," *Electrochem. Soc.*, pp. 39–43, 2015.

[49] N. Barilo and S. Loosen, "Hydrogen Fuel Cells and Fuel Cell Electric Vehicles," *Green Transportation Summit*, 2018. [Online]. Available: http://h2tools.org. [Accessed: 02-Dec-2018].

[50] N. L. Garland, D. C. Papageorgopoulos, and J. M. Stanford, "Hydrogen and fuel cell technology: Progress, challenges, and future directions," *Energy Procedia*, vol. 28, pp. 2–11, 2012.

[51] D. L. Greene, "Status and Prospects of the Global Automotive Fuel Cell Industry and Plans for Deployment of Fuel Cell Vehicles and Hydrogen Refueling Infrastructure Prepared by," 2013.

[52] "The Strategic Cooperation Between Daimler and the Renault-Nissan Alliance Forms Agreement with Ford to Accelerate Commercialization of Fuel Cell Electric Vehicle Technology," *Nissan News*, 2017. [Online]. Available: https://nissannews.com/en-US/nissan/usa/releases/the-strategic-cooperation-

between-daimler-and-the-renault-nissan-alliance-forms-agreement-with-ford-to-accelerate-commercialization-of-fuel-cell-electric-vehicle-technology?mode=print. [Accessed: 03-Dec-2018].

[53] "Global Hydrogen Fuel Cell Vehicles Report 2018: Major Players and Product Rollouts with Detailed Analysis of Plans and Strategies," *Research and Markets*, 2018. [Online]. Available: https://www.prnewswire.com/news-releases/global-hydrogen-fuel-cell-vehicles-report-2018-major-players-and-product-rollouts-with-detailed-analysis-of-plans-and-strategies-300619289.html. [Accessed: 03-Dec-2018].

[54] J. Arboleda, "NEXO-Hyundai Motor España," 2018.

[55] N. American Development and U. European, "Hyundai's Global Approach Asian Development / Korea."

[56] "Hyundai Announces Partnership With Audi On Fuel Cell Technology," *INSIDEEVs*, 2018. [Online]. Available: https://insideevs.com/hyundai-audi-fuel-cell-technology/. [Accessed: 03-Dec-2018].

[57] J. Kurtz, C. Ainscough, G. Saur, S. Sprik, and S. Onorato, "Fuel Cell Electric Vehicle Evaluation," 2018.

[58] C. J. Cleveland and C. Morris, "Fuel Cells," *Handb. Energy*, pp. 323–332, 2014.

[59] FuelCellToday, "Fuel Cell Electric Vehicles: The Road Ahead," 2013.

[60] N. L. Garland, D. C. Papageorgopoulos, and J. M. Stanford, "Hydrogen and fuel cell technology: Progress, challenges, and future directions," in *Energy Procedia*, 2012.

[61] "NPTEL Phase-II: Fuel Cell Technology," 2017. [Online]. Available: https://nptel.ac.in/courses/103102015/introduction and overview of fuel cell/basic electrochemistry for all the fuel cells.html. [Accessed: 03-Dec-2018].

[62] M. Secanell, R. Songprakorp, N. Djilali, and A. Suleman, "Optimization of a proton exchange membrane fuel cell membrane electrode assembly," *Struct. Multidiscip. Optim.*, 2010.

[63] T. Suzuki, H. Murata, T. Hatanaka, and Y. Morimoto, "Analysis of the Catalyst

Layer of Polymer Electrolyte Fuel Cells," 2014.

[64] L. Hamers, "Built for SPEED: More sustainable approaches could get reactions moving," *Sci. News*, 2017.

[65] T.-L. Leon Yu, "Structures of Membrane Electrode Assembly Catalyst Layers for Proton Exchange Membrane Fuel Cells," *Open Fuels Energy Sci. J.*, 2012.

[66] M. A. Fraga, E. Jordão, M. J. Mendes, M. M. A. Freitas, J. L. Faria, and J. L. Figueiredo, "Properties of carbon-supported platinum catalysts: Role of carbon surface sites," *J. Catal.*, vol. 209, no. 2, pp. 355–364, 2002.

[67] C. He, S. Desai, G. Brown, and S. Bollepalli, "PEM Fuel Cell Catalysts: Cost, Performance, and Durability," *Electrochem. Soc.*, 2015.

[68] "Hydrogen fuel cells for the development of a sustainable society," 2017.

[69] H. Wang *et al.*, "Direct and continuous strain control of catalysts with tunable battery electrode materials," *ScienceMag*, vol. 354, no. 6315, 2016.

[70] M. Brodt, R. Wycisk, N. Dale, and P. Pintauro, "Power Output and Durability of Electrospun Fuel Cell Fiber Cathodes with PVDF and Nafion/PVDF Binders," *J. Electrochem. Soc.*, vol. 163, no. 5, pp. F401–F410, 2016.

[71] C. Zhu *et al.*, "Efficient Synthesis of MCu (M = Pd, Pt, and Au) Aerogels with Accelerated Gelation Kinetics and their High Electrocatalytic Activity," *Adv. Mater.*, vol. 28, no. 39, pp. 8779–8783, 2016.

[72] Y. T. Teng and F. C. Wang, "Cost analyses and optimization of a PEMFC electric vehicle model," *SII 2016 - 2016 IEEE/SICE Int. Symp. Syst. Integr.*, vol. 00001, pp. 887–892, 2017.

[73] P. Zelenay, "State of the Art of PGM-free Catalyst Activity and Durability," 2017.

[74] A. Baroutaji, J. G. Carton, M. Sajjia, and A. G. Olabi, "Materials in PEM Fuel Cells," *Ref. Modul. Mater. Sci. Mater. Eng.*, pp. 1–11, 2016.

[75] A. Kongkanand and M. F. Mathias, "The Priority and Challenge of High-Power

Performance of Low-Platinum Proton-Exchange Membrane Fuel Cells,” *J. Phys. Chem. Lett.*, vol. 7, no. 7, pp. 1127–1137, 2016.

[76] A. Steinbach, “High Performance, Durable, Low Cost Membrane Electrode Assemblies for Transportation Applications 2014 Annual Merit Review DOE Hydrogen and Fuel Cells and Vehicle Technologies Programs,” 2014.

[77] A. Kongkanand, “High-Activity Dealloyed Catalysts Anu Kongkanand and Fred Wagner (retired 2012) General Motors Global Product Development, Fuel Cell Activities,” 2014.

[78] B. N. Popov, “Development of Ultra-low Doped-Pt Cathode Catalysts for PEM Fuel Cells (PHASE II) 2015 DOE Hydrogen and Fuel Cells Program Review Project ID # FC088,” 2015.

[79] P. Zelenay, “Hydrogen and Fuel Cells Program Annual Merit Review-Slide 1 Hydrogen and Fuel Cells Program 2016 Annual Merit Review and Peer Evaluation Meeting,” 2016.

[80] V. K. Mathur and J. Crawford, “Fundamentals of gas diffusion layers in PEM fuel cells,” in *Recent Trends in Fuel Cell Science and Technology*, 2007.

[81] H. Sadeghifar, N. Djilali, and M. Bahrami, “Effect of Polytetrafluoroethylene (PTFE) and micro porous layer (MPL) on thermal conductivity of fuel cell gas diffusion layers: Modeling and experiments,” *J. Power Sources*, 2014.

[82] D. Banham and S. Ye, “Current status and future development of catalyst materials and catalyst layers for proton exchange membrane fuel cells: An industrial perspective,” *ACS Energy Lett.*, vol. 2, no. 3, pp. 629–638, 2017.

[83] X. Yu and S. Ye, “Recent advances in activity and durability enhancement of Pt/C catalytic cathode in PEMFC,” *J. Power Sources*, vol. 172, no. 1, pp. 145–154, Oct. 2007.

[84] F. C. Wang and W. H. Fang, “The development of a PEMFC hybrid power electric vehicle with automatic sodium borohydride hydrogen generation,” *Int. J. Hydrogen*

Energy, vol. 42, no. 15, pp. 10376–10389, 2017.

[85] T. Yoshida and K. Kojima, "Toyota MIRAI Fuel Cell Vehicle and Progress Toward a Future Hydrogen Society," *Interface Mag.*, vol. 24, no. 2, pp. 45–49, Jan. 2015.

[86] C. Xu, M. A. Hoque, G. Chiu, T. Sung, and Z. Chen, "Stabilization of platinum-nickel alloy nanoparticles with a sulfur-doped graphene support in polymer electrolyte membrane fuel cells," *RSC Adv.*, vol. 6, no. 113, pp. 112226–112231, 2016.

[87] B. Han *et al.*, "Record activity and stability of dealloyed bimetallic catalysts for proton exchange membrane fuel cells," *Energy Environ. Sci.*, vol. 8, no. 1, pp. 258–266, 2015.

[88] X. Tian *et al.*, "Transition Metal Nitride Coated with Atomic Layers of Pt as a Low-Cost, Highly Stable Electrocatalyst for the Oxygen Reduction Reaction," *J. Am. Chem. Soc.*, vol. 138, no. 5, pp. 1575–1583, Feb. 2016.

[89] K. A. Kuttiyiel *et al.*, "Enhancement of the oxygen reduction on nitride stabilized pt-M (M=Fe, Co, and Ni) core–shell nanoparticle electrocatalysts," *Nano Energy*, vol. 13, pp. 442–449, Apr. 2015.

[90] M. Oezaslan, F. Frédé, F. H. Hasché, and P. Strasser, "Pt-Based Core−Shell Catalyst Architectures for Oxygen Fuel Cell Electrodes," *J. Phys. Chem. Lett*, vol. 4, p. 3291, 2013.

[91] V. R. Stamenkovic *et al.*, "Improved Oxygen Reduction Activity on Pt3Ni(111) via Increased Surface Site Availability," *Science (80-.).*, vol. 315, no. 5811, pp. 493–497, Jan. 2007.

[92] S.-I. Choi *et al.*, "Synthesis and Characterization of 9 nm Pt–Ni Octahedra with a Record High Activity of 3.3 A/mg $_{Pt}$ for the Oxygen Reduction Reaction," *Nano Lett.*, vol. 13, no. 7, pp. 3420–3425, Jul. 2013.

[93] J. H. Wee, K. Y. Lee, and S. H. Kim, "Fabrication methods for low-Pt-loading electrocatalysts in proton exchange membrane fuel cell systems," *J. Power Sources*,

vol. 165, no. 2, pp. 667–677, 2007.

[94] H. Su, T. C. Jao, O. Barron, B. G. Pollet, and S. Pasupathi, “Low platinum loading for high temperature proton exchange membrane fuel cell developed by ultrasonic spray coating technique,” *J. Power Sources*, vol. 267, pp. 155–159, 2014.

[95] A. D. Taylor, E. Y. Kim, V. P. Humes, J. Kizuka, and L. T. Thompson, “Inkjet printing of carbon supported platinum 3-D catalyst layers for use in fuel cells,” *J. Power Sources*, vol. 171, no. 1, pp. 101–106, 2007.

[96] C. Spiegel, “Polarization Curves,” *Fuel Cell Basics*, 2017. [Online]. Available: https://www.fuelcellstore.com/blog-section/polarization-curves. [Accessed: 20-Apr-2019].

[97] K. Takahashi, K. Kakinuma, and M. Uchida, “Improvement of Cell Performance in Low-Pt-Loading PEFC Cathode Catalyst Layers Prepared by the Electrospray Method,” *J. Electrochem. Soc.*, vol. 163, no. 10, pp. F1182–F1188, 2016.

[98] Z. Qi and A. Kaufman, “Improvement of water management by a microporous sublayer for PEM fuel cells,” *J. Power Sources*, 2002.

[99] N. Kumano, K. Kudo, A. Suda, Y. Akimoto, M. Ishii, and H. Nakamura, “Controlling cracking formation in fuel cell catalyst layers,” *J. Power Sources*, vol. 419, no. March, pp. 219–228, 2019.

[100] S. Park, J.-W. Lee, and B. N. Popov, “A review of gas diffusion layer in PEM fuel cells: Materials and designs,” *Int. J. Hydrogen Energy*, vol. 37, no. 7, pp. 5850–5865, Apr. 2012.

ANNEXES

Annex 1 Polymer electrolyte membrane (PEMFCs)

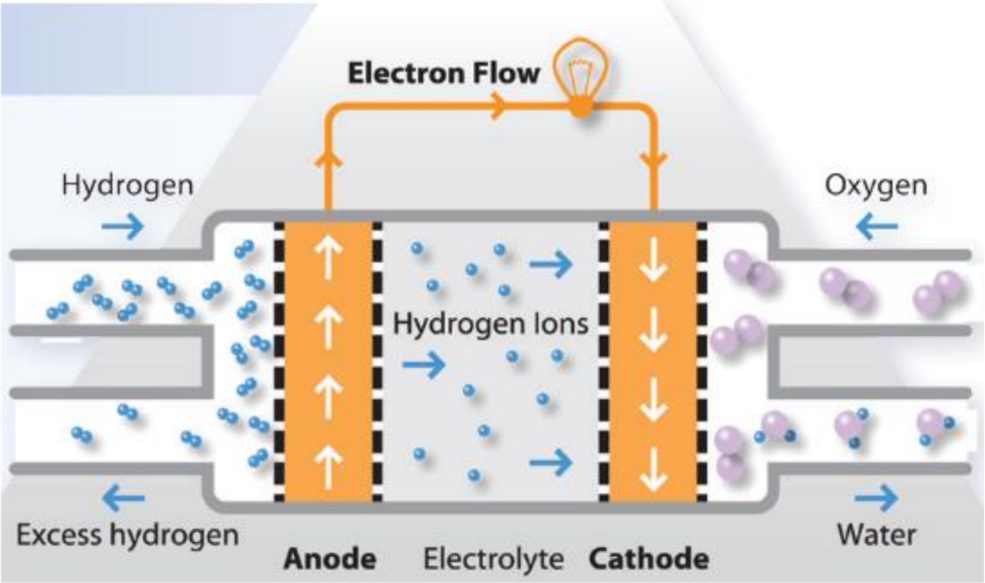

Annex 2 Direct Methanol (DMFCs)

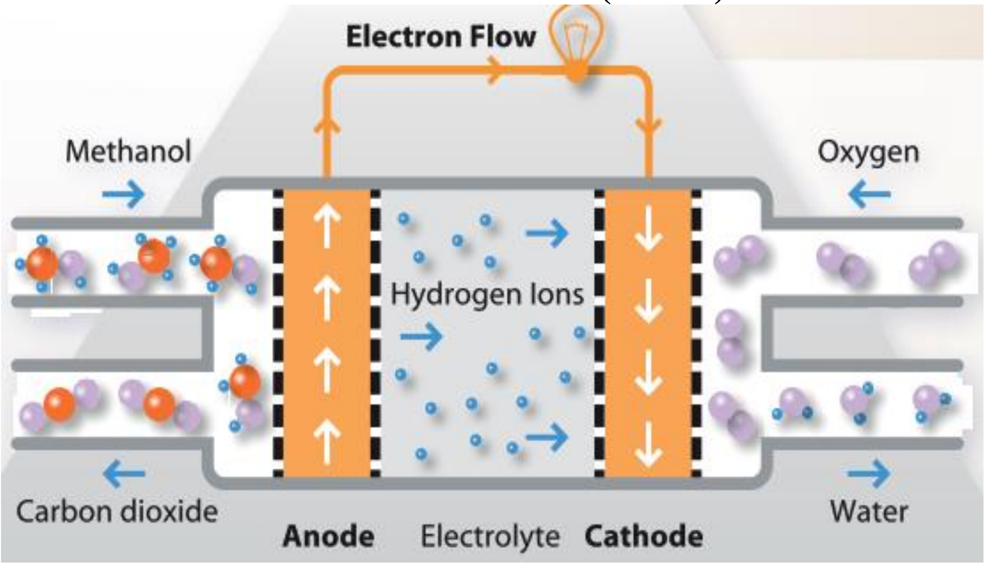

Annex 3 Alkaline electrolyte (AFCs)

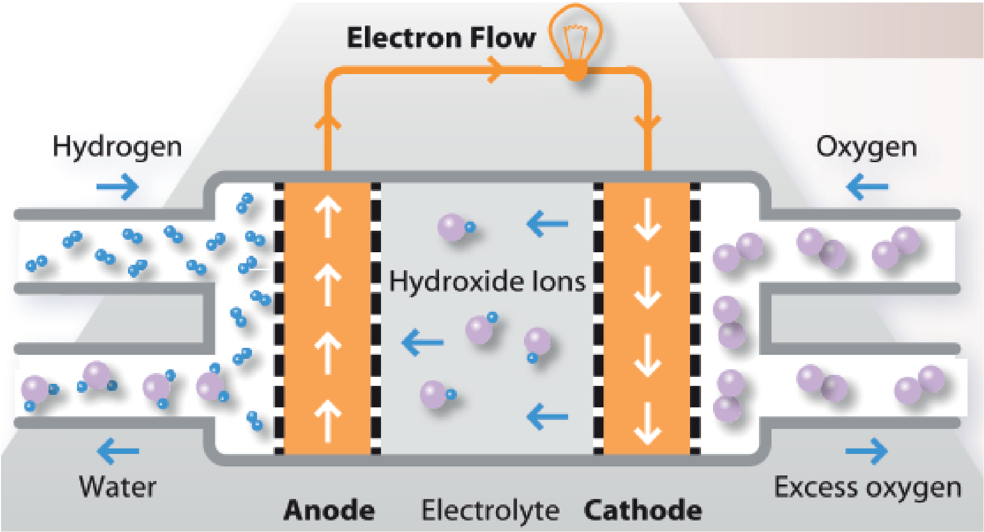

Annex 4 Phosphoric acid (PAFCs)

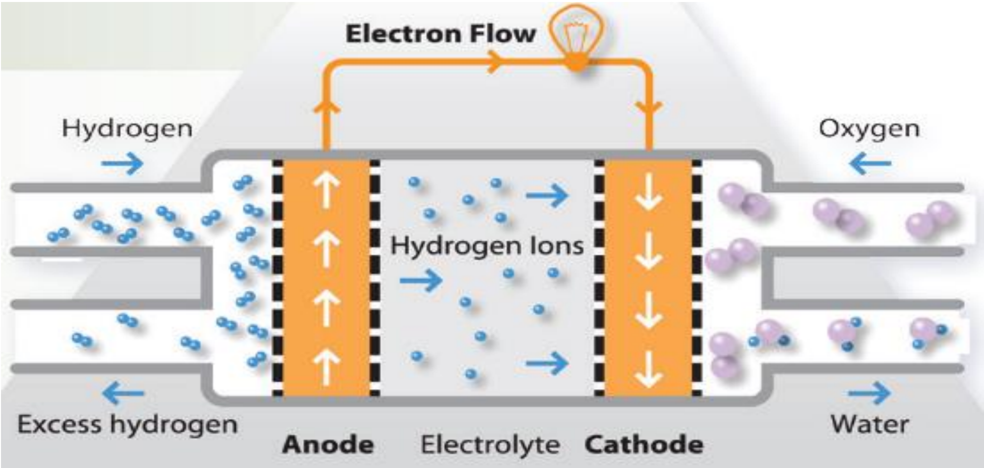

Annex 5 Molten carbonate (MCFCs)

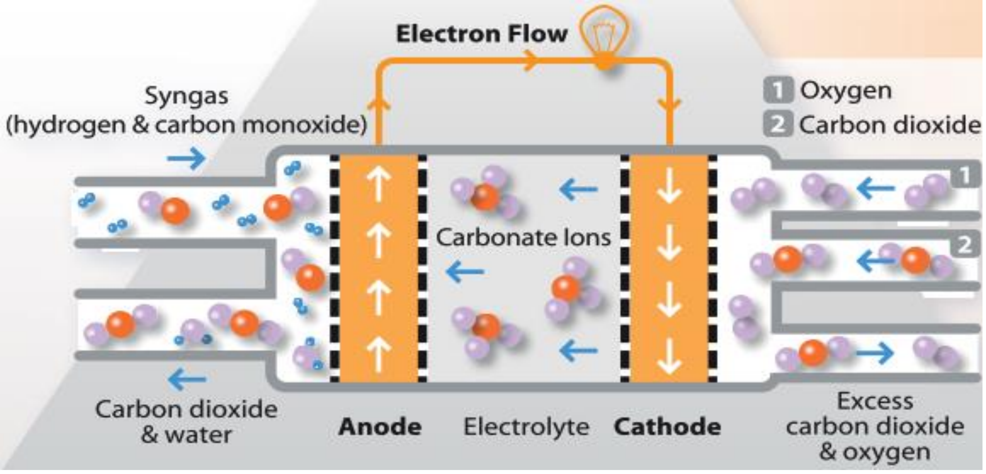

Annex 6 Solid oxide (SOFCs)

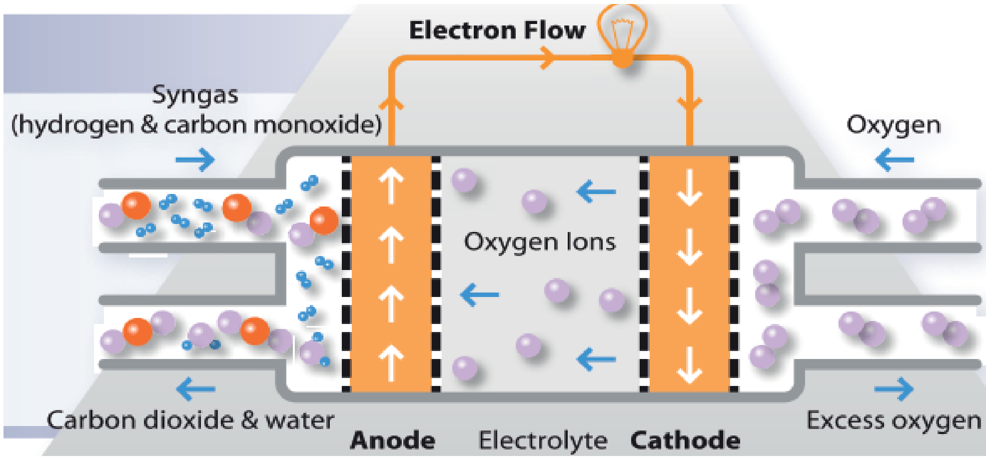

Annex 7 Repeatable polarization curves at 50% RH of 3 cells

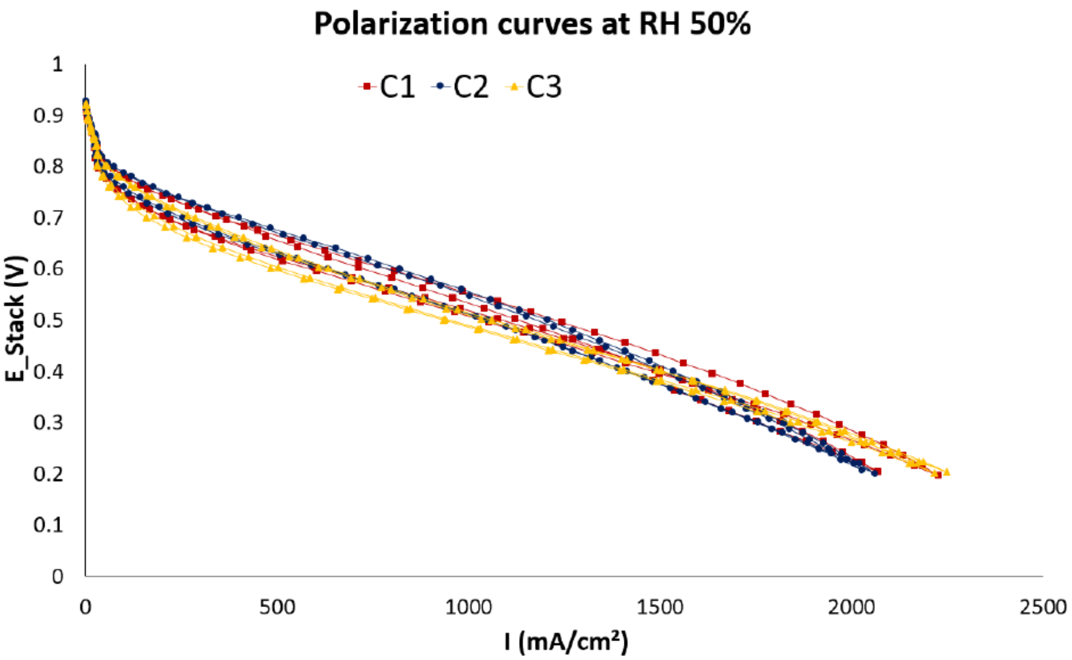

Annex 8 Repeatable cyclic voltammograms at 30°C of 3 cells

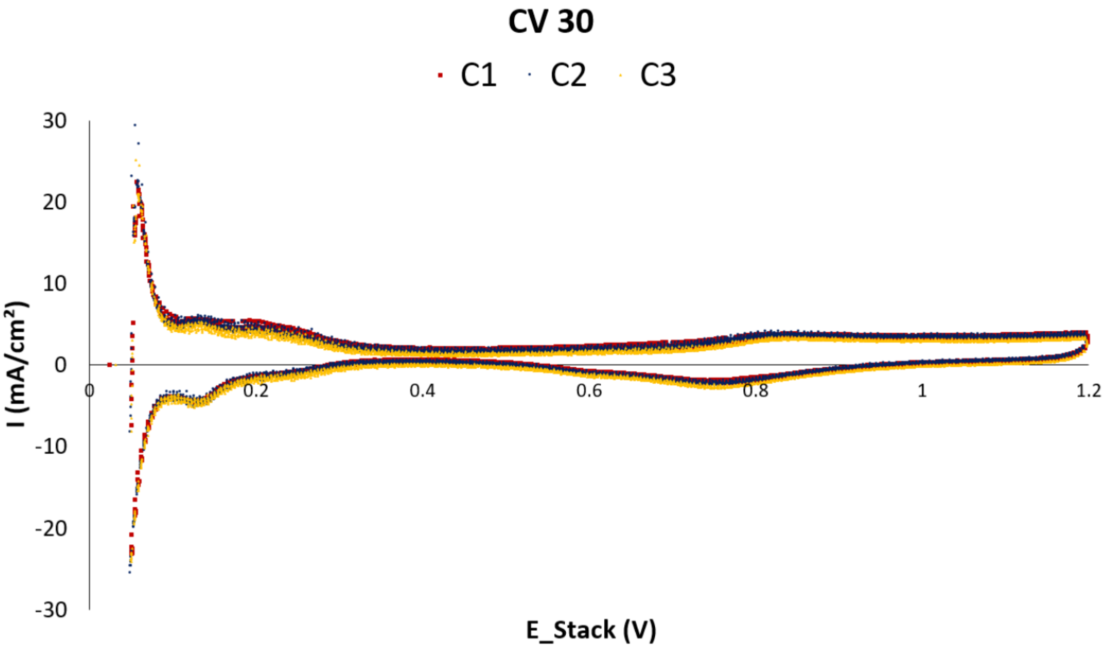

Annex 9 Cell resistance from polarization curve at 50% RH

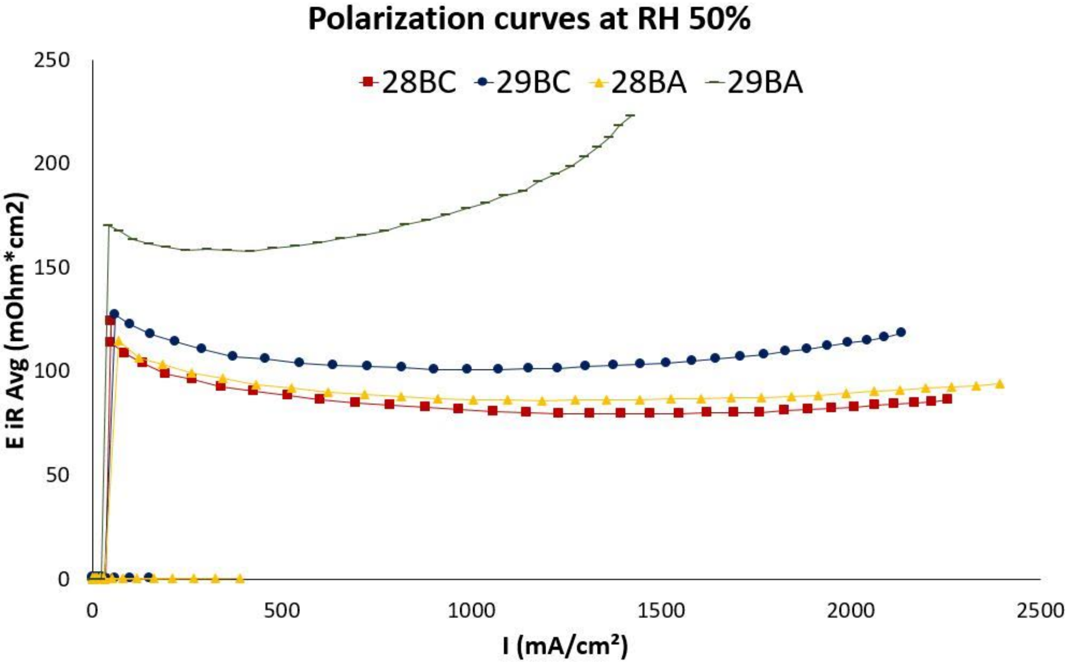

Annex 10 Cell resistance from polarization curve at 70% RH

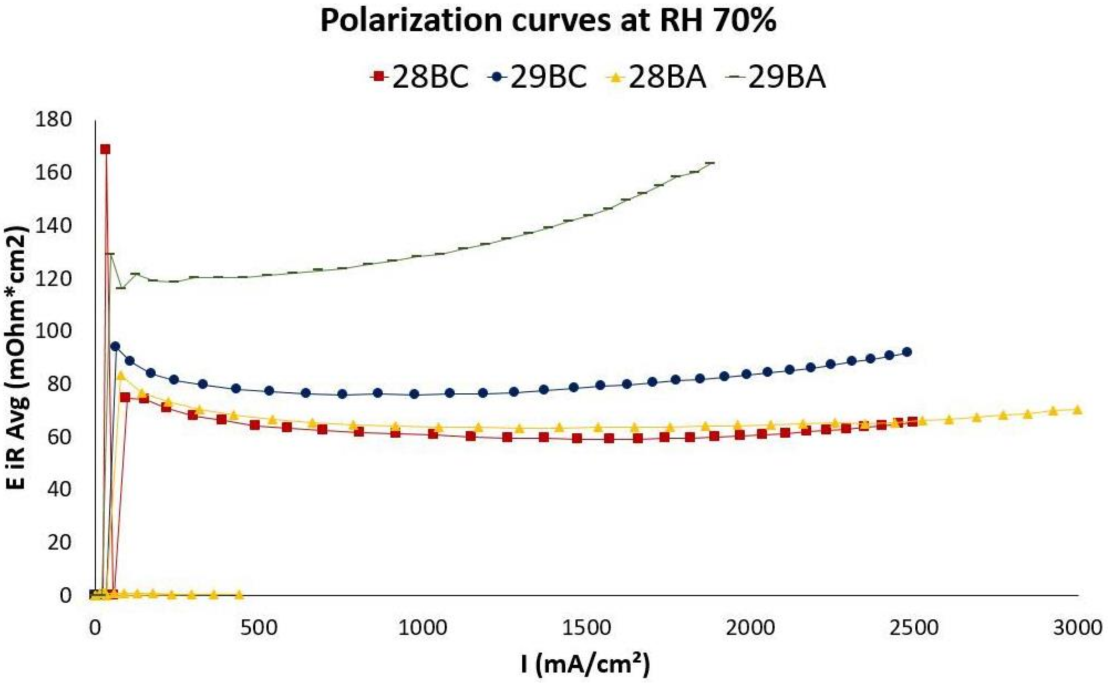

Annex 11 Cell resistance from polarization curve at 90% RH

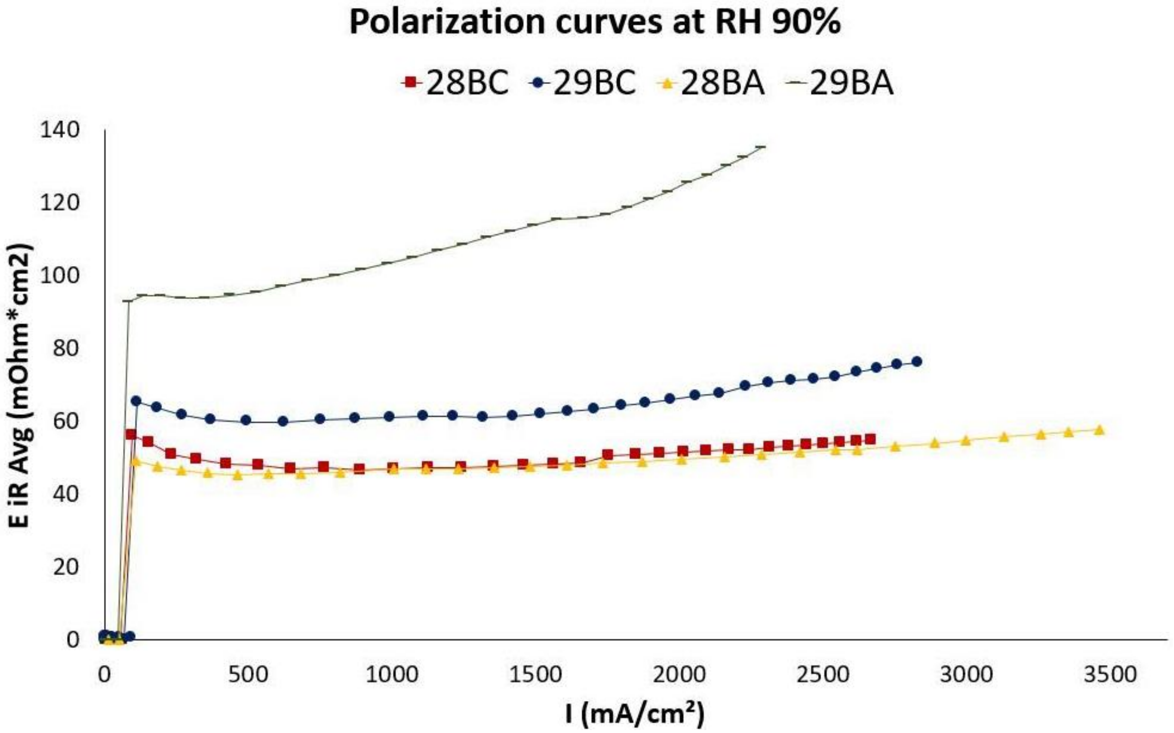

Annex 12 Limiting current experiment with GDL 28 BC

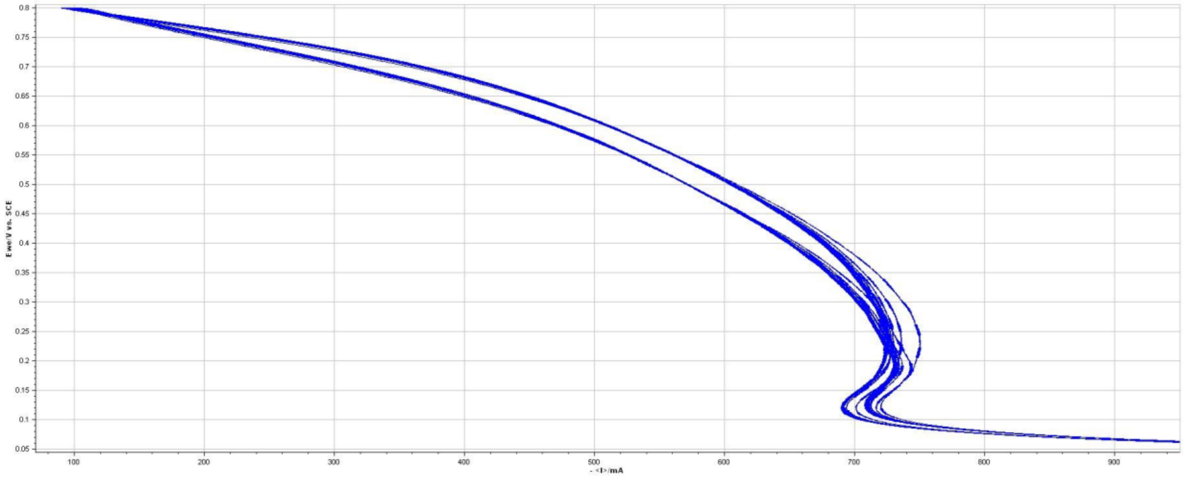

Annex 13 Limiting current experiment with GDL 29 BC

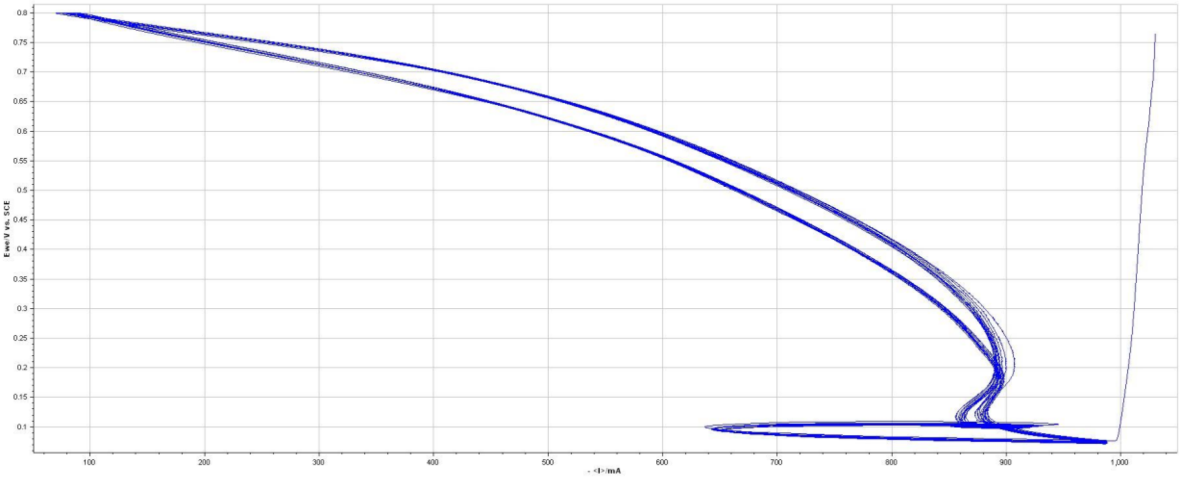

Annex 14 Limiting current experiment with GDL 28 BA

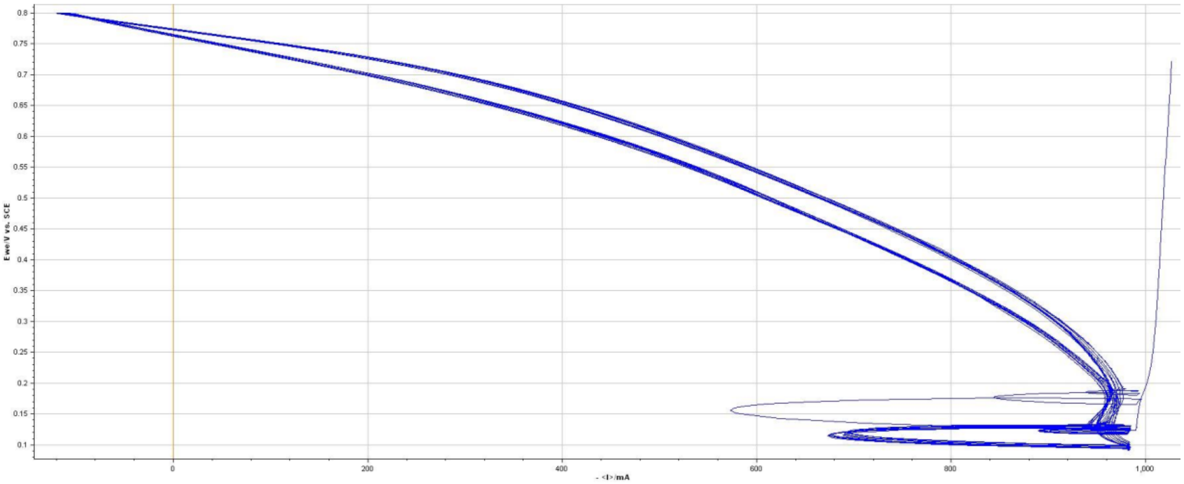

Annex 15 Limiting current experiment with GDL 29 BA

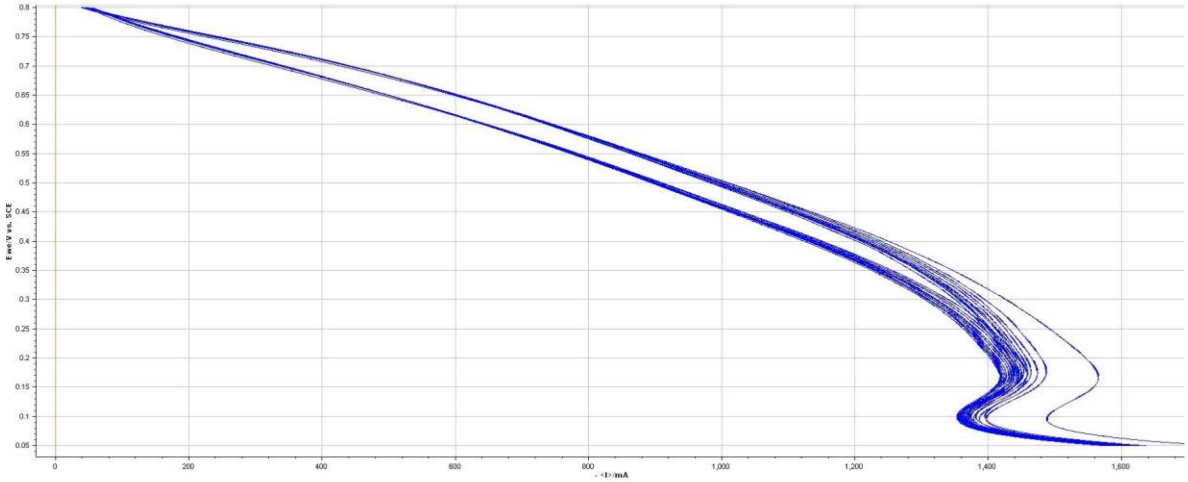

Annex 16 Pore size distribution SIGRACET® GDL BA series

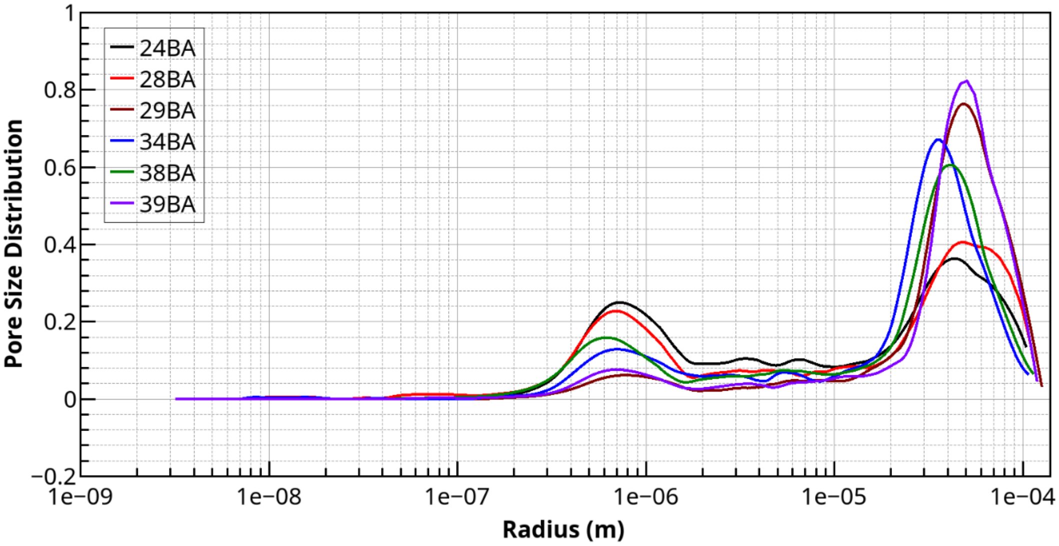

Annex 17 Pore size distribution SIGRACET® GDL BC series